Palacký University Olomouc

Faculty of Science

Department of Cell Biology and Genetics

A comparative study of Tau R2 and R3 aggregates on tau seeding in neurodegenerative diseases

Master Thesis

Bc. Jiří Hrubý

Study program: Biology

Field of Study: Molecular and Cell Biology

Form of Study: Full-time

Olomouc 2022 **Supervisor: Mgr. Viswanath Das, Ph.D**

UNIVERZITA PALACKÉHO V OLOMOUCI

Přírodovědecká fakulta

Akademický rok: 2020/2021

ZADÁNÍ DIPLOMOVÉ PRÁCE

(projektu, uměleckého díla, uměleckého výkonu)

Jméno a příjmení:	**Bc. Jiří HRUBÝ**
Osobní číslo:	**R20907**
Studijní program:	**N1501 Biologie**
Studijní obor:	**Molekulární a buněčná biologie**
Téma práce:	**Komparativní studie vlivu Tau R2 a R3 agregátů na seeding tau u neurodegenerativních onemocnění**
Zadávající katedra:	**Katedra buněčné biologie a genetiky**

Zásady pro vypracování

Tauopathies are a group of neurodegenerative diseases characterized by the abnormal deposition of tau protein in the brain. The exact mechanisms of tau pathology induction are still yet to be elucidated. This study will use exogenous Tau R2 and R3 aggregates to investigate differences in intracellular tau seeding, a potential mechanism leading to tau pathology, using synthetic peptides of tau, Tau RD P301S biosensor cells, fluorescent microscopy and Western blotting.

Rozsah pracovní zprávy:
Rozsah grafických prací:
Forma zpracování diplomové práce: **tištěná**
Jazyk zpracování: **Angličtina**

Seznam doporučené literatury:

Antitumour drugs targeting Tau R3 VQIVYK and Cys322 Prevent Seeding of endogenous Tau aggregates by Exogenous Seeds. The FEBS Journal. 2021, 289:1929-1949.
Tau secretion and propagation: perspectives for potential preventive interventions in Alzheimer's disease and other tauopathies. Experimental Neurology. 2021, 343:113756.
Biophysical properties of a tau seed. Sci Rep. 2021 Jun 30;11(1):13602.
Quantitative Methods for the Detection of Tau Seeding Activity in Human Biofluids. Frontier in Neuroscience. 2021 Mar 19;15:654176. doi: 10.3389/fnins.2021.654176.

Vedoucí diplomové práce: **Mgr. Viswanath Das, PhD.**
Ústav molekulární a translační medicíny

Datum zadání diplomové práce: **29. října 2020**
Termín odevzdání diplomové práce: **31. července 2022**

L.S.

doc. RNDr. Martin Kubala, Ph.D.
děkan

prof. RNDr. Zdeněk Dvořák, DrSc.
vedoucí katedry

21 -04- 2022

V Olomouci dne 29. října 2020

Bibliographical identification:

Author's first name and surname	Jiří Hrubý
Title	A comparative study of Tau R2 and R3 aggregates on tau seeding in neurodegenerative diseases
Type of thesis	Master
Department	Department of Cell Biology and Genetics
Supervisor	Mgr. Viswanath Das, Ph.D.
The year of presentation	2022
Keywords	Alzheimer's disease, tauopathy, tau protein, aggregates, seeding
Number of pages	viii, 41
Language	English

Summary:

Tau, as a microtubule-associated protein, is important for the proper functions of the CNS. However, its predisposition to misfolding and prion-like properties can trigger neurodegeneration by forming intracellular aggregates of misfolded tau and destabilizing the neuronal cytoskeleton. The creation of tau aggregates preludes neurodegenerative diseases, particularly tauopathies. Dementia resulting in changes in cognitive functions is one of the primary symptoms of neurodegeneration. The number of people with dementia worldwide is in the millions, and this number is on the rise as the world population ages, with many cases remaining undiagnosed. Therefore, to facilitate research, diagnostics, and treatment development, it is crucial to develop reliable tauopathy models to better understand neurodegeneration mechanisms *in vitro*. We conducted a comparative study of two tau peptide fibrils, R2 and R3, used in the research of tauopathies. Their seeding activity in cell cultures was observed using western blotting and fluorescent microscopy. Our findings suggest that fibrils of both peptide types display comparable properties: (1) successfully induce seeding by inducing tau aggregation *in vitro* at a similar concentration range (minimal concentration) and (2) seed the aggregation of native tau in cell models with the same potency. However, R2 aggregates were found to induce intracellular aggregation faster and more efficiently. The results presented in this thesis offer fresh perspectives on the processes of tau seeding and will help further research on tauopathies.

Bibliografická identifikace:

Jméno a příjmení autora	Jiří Hrubý
Název práce	Komparativní studie vlivu Tau R2 a R3 agregátů na seeding tau u neurodegenerativních onemocnění
Typ práce	Diplomová
Pracoviště	Katedra buněčné biologie a genetiky
Vedoucí práce	Mgr. Viswanath Das, Ph.D.
Rok obhajoby práce	2022
Klíčová slova	Alzheimerova choroba, tauopatie, tau, proteinové agregáty, seeding
Počet stran	viii, 41
Jazyk	angličtina

Souhrn:

Tau jako protein asociovaný s mikrotubuly je důležitý pro správné funkce CNS. Kvůli predispozici k chybnému skládání a prion-like vlastnostem však může vyvolat neurodegeneraci tvorbou intracelulárních agregátů chybně složeného tau a destabilizací neuronového cytoskeletu. Tvorba agregátů tau předchází neurodegenerativním onemocněním, zejména tauopatiím. Demence vedoucí ke změnám kognitivních funkcí je jedním z primárních symptomů neurodegenerace. Počet lidí s demencí na celém světě je v milionech a toto číslo roste s tím, jak světová populace stárne, přičemž mnoho případů zůstává nediagnostikováno. Pro usnadnění výzkumu, diagnostiky a vývoje léčby je proto zásadní vyvinout spolehlivé modely tauopatie, aby bylo možné lépe porozumět mechanismům neurodegenerace *in vitro*. Provedli jsme srovnávací studii dvou tau peptidových fibril, R2 a R3, používaných při výzkumu tauopatií. Jejich seeding v buněčných kulturách byl pozorován pomocí western blotu a fluorescenční mikroskopie. Naše zjištění naznačují, že fibrily obou typů peptidů vykazují srovnatelné vlastnosti: (1) úspěšně indukují seeding indukcí agregace tau *in vitro* v podobném koncentračním rozmezí (minimální koncentrace) a (2) seedují agregaci nativního tau v buněčných modelech se stejnou potencí. Bylo však zjištěno, že agregáty R2 indukují intracelulární agregaci rychleji a účinněji. Výsledky prezentované v této práci nabízejí nové pohledy na procesy seeding tau a pomohou dalšímu výzkumu tauopatií.

"I declare that this Master Thesis was developed independently, under the guidance of my supervisor, and by using the cited literature."

In Olomouc, …….…….. Signature …….……..

ACKNOWLEDGMENT

This Master's thesis was performed at the Institute of Molecular and Translational Medicine in Olomouc, in collaboration with Palacký University in Olomouc.

First, I would like to thank my supervisor, Mgr. Viswanath Das, Ph.D., for his patience with me through my work on this thesis, his friendly attitude, valuable guidance and insight and his support, and Mgr. Narendran Annadurai. Both taught me new skills and techniques, advised me during experiments and uplifted me during times of need, for which I am grateful. I would also like to thank Mgr. Anna Janoštáková and Bc. Renata Buriánová for their friendly attitude and whose advice and support in the laboratory were invaluable. And finally, I would like to thank my family and friends for their support during my studies.

TABLE OF CONTENTS

LIST OF ABBREVIATIONS

0N/1N/2N	Number of N-terminal domain inserts of tau protein
3R/4R	Number of microtubule-binding domain repeats of tau protein
AD	Alzheimer's disease
CBD	Corticobasal dementia
HDAC6	Histone deacetylase 6
MAPT	Microtubule-associated protein tau
MBD	Microtubule binding domain of tau protein
N1/N2	Distinct N-terminal domain inserts of tau protein
NFTs	Neurofibrillary tangles
PD	Parkinson's disease
PHFs	Paired helical filaments
PiD	Pick's disease
PTMs	Post-translational modifications
PSP	Progressive supranuclear palsy
R1/R2/R3/R4	Distinct microtubule-binding domain repeats of tau protein
Sirt1	Sirtuin 1

LIST OF FIGURES

LIST OF TABLES

1 INTRODUCTION

As presented in World Alzheimer Report 2021 (Gauthier *et al.*, 2021), dementia is the 7th leading cause of mortality worldwide. There are ca. 55 million people afflicted with dementia globally, and this number is rising rapidly as the world population ages and correlates with ageing populations, especially in highly developed countries. Alarmingly, it is estimated that less than 25 % of the population suffering from dementia is accurately diagnosed, and even less in countries with a low socio-demographic index. Alzheimer's disease (AD) is the leading cause of dementia and is characterized by the accumulation of aggregates of misfolded amyloid-beta and tau proteins (Abubakar *et al.*, 2022). The microtubule-associated tau protein is crucial for proper cytoskeletal functions in neurons, and therefore, its pathology can severely affect the central nervous system (CNS).

Misfolded tau in tauopathies – a group of CNS diseases with aberrant tau protein – like AD, frontotemporal dementia, Pick's disease and corticobasal degeneration exhibit prion-like properties, recruiting unfolded native proteins into a misfolded state, leading to the accumulation of misfolded protein aggregates. These aggregates can spread intercellularly and seed the aggregation of the native protein in previously healthy neurons. Therefore, to study, diagnose and treat tauopathies, it is important to develop reliable tauopathy models (Lathuiliere and Hyman, 2021) and understand processes in the *in vitro* conditions to allow the best extrapolation of the conditions *in vivo* in preclinical models for eventually interventions in patients. With no effective treatment available (Abubakar *et al.*, 2022) and a rising number of people afflicted with neurodegenerative tauopathies, we decided to conduct a comparative study of the effects of tau aggregates using peptides of repeat 2 (R2) and repeat 3 (R3) of tau microtubule-binding domain to better understand the process of seeding and to reveal possible targets for drug development.

2 AIM OF THESIS

The aim of this master thesis is to compare the seeding activity of exogenous tau R2 and R3 aggregates on the induction of intracellular seeding in a cellular model (biosensor cells) of tau aggregation expressing aggregation-prone Tau-RD-P301S by Western blotting and fluorescent microscopy.

3 LITERATURE REVIEW

3.1 Microtubule-associated protein tau in health

3.1.1 Genetics of tau

Tau (**t**ubulin-**a**ssociated **u**nit) is an important cytoskeletal microtubule-associated protein, abundantly expressed in cells of the CNS, especially in axons of neurons, but also in somas and dendrites (Zeng *et al., 2021*). Tau is also found in other cellular compartments, including the plasma membrane, nucleus, and mitochondria, and other tissues and organs, such as salivary glands, pancreas, breasts, kidneys, testes and in both hearth and skeletal muscle (Guo *et al.*, 2017; Liang *et al.*, 2022). It is encoded by the *MAPT* gene on chromosome 17q21 (Neve *et al.*, 1986), which consists of sixteen exons (Muralidar *et al.*, 2020). Three of these exons (E2, E3 and E10) undergo alternative splicing to give rise to six isoforms of tau (Fig. 1). Furthermore, exons E4A, E6 and E8 are skipped in CNS and transcribed only in peripheral nerves, and exon E0 E14 is a part of 3' untranslated region of mRNA. After transcription, tau mRNA is transported to the proximal part of the axons for protein translation to occur. This enhances the polarity of neuronal cells (Guo *et al.*, 2017, Muralidar *et al.*, 2020). Two haplotypes of the *MAPT* gene exist, H1 and H2, distinguished by an inverted or non-inverted sequence of the genes on chromosomes (Zhang *et al.*, 2018).

3.1.2 Structure of tau

Tau protein comprises four distinct regions: the N-terminal domain, the proline-rich domain, the microtubule-binding domain (MBD) and the C-terminal domain. (Zeng *et al.*, 2021). Alternative splicing of tau mRNA results in six isoforms in humans, 0N3R, 1N3R, 2N3R, 0N4R, 1N4R and 2N4R, which are distinguished based on the presence of 0, 1 or 2 repeats in N-terminal domain (0-2N) and 3 or 4 repeats in MBD (3R or 4R) (Muralidar *et al.*, 2020; Zeng *et al.*, 2021). MBD repeats are followed by the "fifth repeat region" R' located downstream of the repeat region (Fig 1), which enhances the binding of full-length (2N4R) tau to tubulin (Liang *et al.*, 2022). The expression of different isoforms is ontogenetically dependent – all six isoforms are present in the adult human brain, whereas human fetal brains express only 0N3R. In healthy adults, 3R and 4R isoforms expression should be at a 1:1 ratio (Guo *et al.*, 2017; Muralidar *et al.*, 2020). The isoform expression can also vary in different cerebral regions (Guo *et al.*, 2017).

Tau is an intrinsically disordered protein of flexible conformation and forms transient secondary but no tertiary structures. The MBD repeats assemble into β-sheets due to the presence of two hexapeptide sequences, PH6* (^{275}VQIINK^{280}) in R2 and PH6 (^{306}VQIVYK^{311}) in R3(Fig. 1), and polyproline II helices in the proline-rich domain (Zeng *et al.*, 2021). Tau is a polyelectrolyte molecule with positively charged inner regions (proline-rich domain and MBD) and negatively charged terminal domains. Therefore, a "paper-clip" conformation was proposed and is widely accepted in free tau, with C-terminus folding over MBD and N-terminal domain folding over C-terminus (Fig. 2). The proximity of both termini in such conformation was suggested by FRET detection and NMR spectroscopy and this conformation is lost upon binding to microtubules, with N-terminal domain projecting away from microtubule (Barbier *et al.*, 2019; Guo *et al.*, 2017; Jeganathan *et al.*, 2006; Mukrasch *et al.*, 2009). The structure of tau is compact in solutions; however, this trait differs between the domains – especially in MBD – and is dependent on their flanking domains. For instance, MBD is more compact when isolated from full-length proteins. MBD also appears to be more rigid than other domains, for example, the N-terminal domain, which is highly mobile (Zeng *et al.*, 2021).

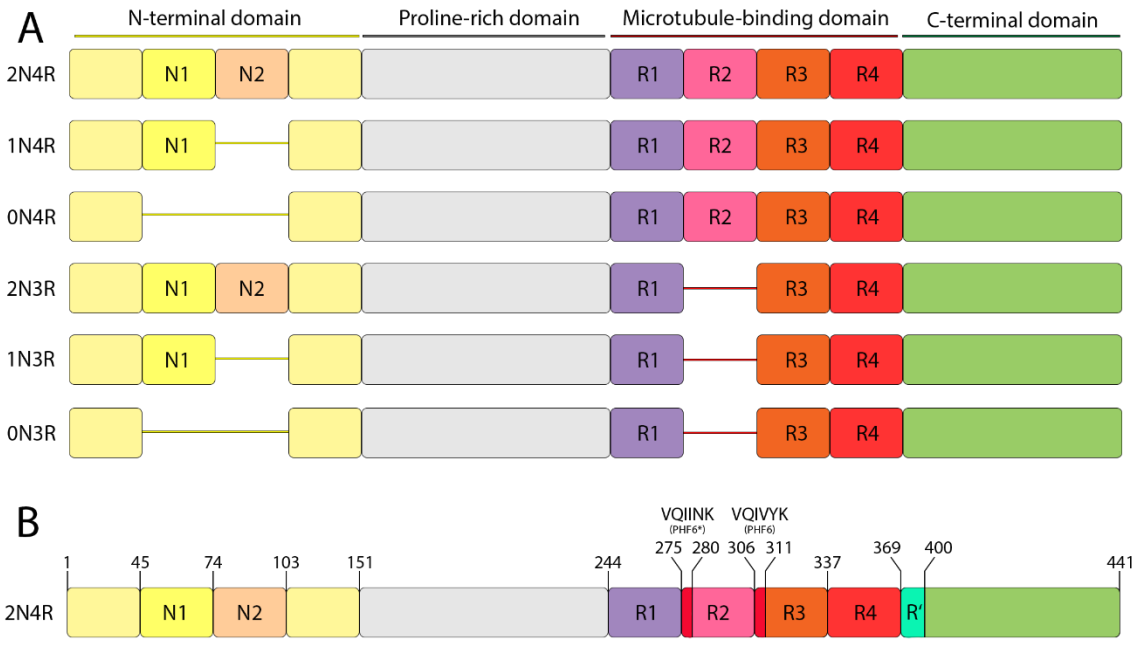

Figure 1: A - schematic drawing of tau isoforms. Different domains are highlighted by distinct colors. B - the longest human tau isoform with the number of flanking amino acids of regions. Aggregation-prone hexapeptide sequences, PH6, PH6*, and microtubule-binding repeat R' are indicated. (Hrubý, 2020, modified)

3.1.3 Physiological functions of tau

The primary function of tau protein is to maintain the dynamicity and stability of microtubules, which ensures a proper cytoskeleton function, especially in distal portions of dendrites and neurons. Aberrant microtubule stability and dynamicity result in loss of microtubule functions due to dissociation of microtubules, resulting in defective axonal transport of cellular cargo (e.g., membranous vesicles with neurotransmitter) and progressively leading to neurodegeneration. The positively charged proline-rich domain is also involved in tau-microtubule interaction by binding to negatively charged microtubule regions (Guo *et al.*, 2017, Muralidar *et al.*, 2020). N-terminal domain, while projecting away from the microtubule (Fig. 2), interacts dynactin complex, which mediates the association of microtubular molecular motor dynein with membranous cargoes, influencing proper cargo transport (Magnani *et al.*, 2007).

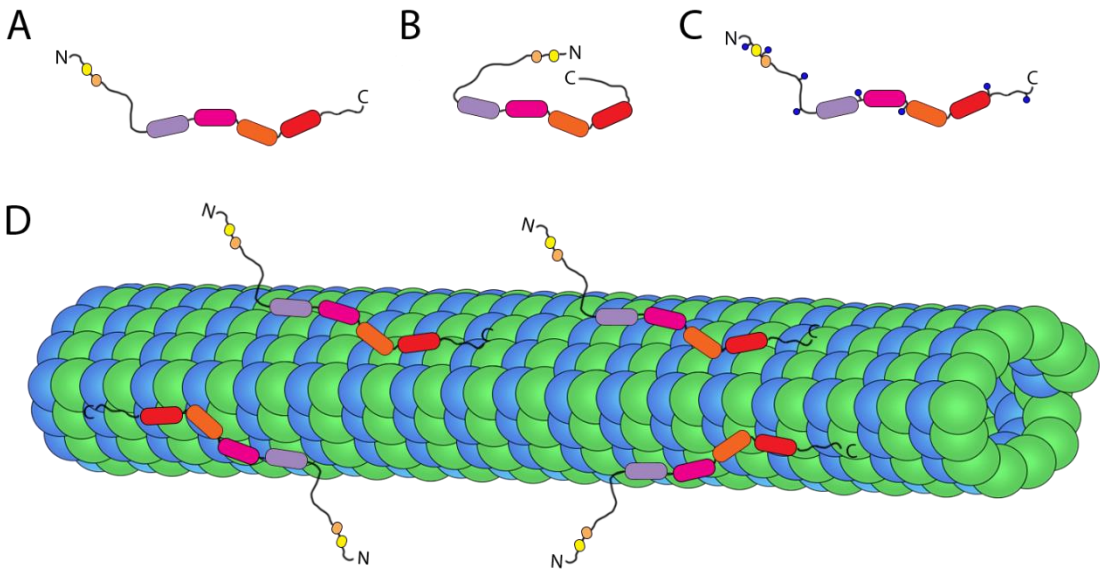

Figure 2: A – a schematic drawing of tau; B – paperclip conformation of free tau; C – phosphorylated free tau. Blue dots indicate phosphate residues; D – tau binding to microtubule with N-terminal domain projecting away (Hrubý, 2020)

However, some studies suggest that in tau-knock-out phenotypes, axonal transport functions are retained (reviewed in Morris *et al.*, 2011). This indicates that tau may not be an essential player in axonal transport but contributes to the process along with other proteins, such as dynein and kinesin. In addition, tau can also induce microtubule assembly (Barbier *et al.*, 2019). The number of MBD repeats linearly determines the binding affinity of tau to microtubules; thus, 3R tau has a lower microtubule-binding

affinity than 4R tau. This concurs with different isoform levels in developing and mature brains. Developing brains have a greater need for neuronal plasticity; thus, shorter tau isoforms are expressed in fetal brains (Barbier *et al.*, 2019; Hanger *et al.*, 2009). Several studies found that the primary function of tau overlaps with that of other microtubule-associated proteins, such as MAP1A, MAP1B and MAP2 (reviews in Bakota *et al.*, 2017). In tau knock-out mice, microtubule stability and functions are not severely hindered, and critical brain functions are preserved. However, it worsened the phenotype in MAP1B knock-out mice, where severe brain dysgenesis with high early lethality occurred. Similar effects were observed in the other two MAPs (Bakota *et al.*, 2017, Takei *et al.*, 2000). Due to the early lethality of knock-out mice, it was not yet possible to study the effects of double knock-out in adult mice. (Takei *et al.*, 2000)

Besides binding microtubules, 4R tau also binds to nuclear DNA through its interactions with histones that stabilize condensed chromatin to make them more compact. Therefore, tau can protect the DNA in a chaperone-like manner or like a heat-shock protein Hsp70 and affect gene expression by binding to AT-rich minor grooves of DNA. This function is disrupted in frontotemporal lobar degeneration (Guo *et al.*, 2017; Rico *et al.*, 2021).

Through MBD, tau can interact with other cell compartments and proteins, such as F-actin, α-synuclein, apolipoprotein E, and presenilin 1 or histone-6-deacetylase (HDAC6) (Guo *et al.*, 2017; Liang *et al.*, 2022; Muralidar *et al.*, 2020). Through interaction with F-actin, tau can cross-link microtubules and actin microfilaments, further affecting the cytoskeleton, and through interaction with HDAC6, it may further affect chromatin structure and gene expression; however, the primary function of this interaction is tubulin deacetylation (Elie *et al.*, 2015).

The N-terminal domain can also interact with other compartments, such as the neural plasma membrane, through interactions with annexin A2 – a membrane-binding protein – and other proteins. N-terminal domain-protein interaction is – similarly to MBD – dependent on the number of N-terminal repeats, where, for example, apolipoprotein A1 preferentially – probably exclusively – binds to 2N tau, whereas β-synuclein and synaptophysin bind to 0N tau. It also affects cellular locality (Guo *et al.*, 2017)

Tau also contributes to signalling pathways by participating in signalling cascades of Src family kinases (e.g., Fyn), phospholipase C-γ, peptidylprolyl cis/trans isomerases (e.g., pin1) or phosphatidylinositol 3-kinase. In these interactions, the proline-rich domain is involved. The proline-rich domain includes seven Pro-X-X-Pro motifs, which serve as recognition sites in these interactions (Guo *et al.*, 2017; Liang *et al.*, 2022). Also, tau appears to be essential for myelination, insulin and neurotrophin receptor signalling, and for signalling in oligodendrocytes (Mueller *et al.*, 2021)

3.1.4 Tau regulation via posttranslational modifications

The biological functions of tau are regulated by various posttranslational modifications. PTMs of tau include phosphorylation, acetylation, nitration, glycation, SUMOylation, ubiquitination, and proteolytic cleavage – truncation. Among these PTMs, the most prevalent and widely studied one is phosphorylation. Imbalance in PTM regulation can lead to tau pathology development (Guo *et al.*, 2017; Mietelska-Porowska *et al.*, 2014)

Kinases responsible for tau phosphorylation are divided into three main groups – proline-directed serine/threonine protein kinases, non-proline directed serine/threonine protein kinases and tyrosine protein kinases. The proline-directed group consists of glycogen synthase kinase-3, cyclin-dependent kinase-5 and C-Jun amino-terminal kinases, and several others, like mitogen-activated protein kinases and stress-activated kinases. The non-proline-directed group includes casein kinase 1, tau-tubulin kinase 1/2, protein kinase A, protein kinase C, dual specificity tyrosine-phosphorylation-regulated kinase 1A, microtubule-affinity regulating kinases, 5'-adenosine monophosphate-activated protein kinase, and others. Lastly, Src, Fyn, Abl or Syk belong to the tyrosine protein kinases group. One enzyme can add phosphate residue on many sites, for example, glycogen synthase kinase-3 on over 40 sites and casein kinase 1 on 46 sites. A proline residue follows nearly 50 % of phosphorylation sites. However, only five sites – Tyr18, Tyr29, Tyr197, Tyr310, and Tyr394 – are the targets of tyrosine protein kinases (Muralidar *et al.*, 2020, Chu and Liu, 2022).

Dephosphorylation of tau is executed mainly by protein phosphatase 2A, which is responsible for 70 % of dephosphorylation in tau. However, other phosphatases interact with phospho-tau (p-tau) as well, such as protein phosphatase 2B, protein phosphatase 1,

protein phosphatase 5 or calcyclin-binding protein and Siah-1 interacting protein (Liang *et al.*, 2022; Liu *et al.*, 2005; Mietelska-Porowska *et al.*, 2014)

Acetylation of tau is another important PTM. The enzyme responsible for adding the acetyl residue is the cAMP response element binding protein-binding protein (CBP), and deacetylation is conducted by sirtuin 1 (Sirt1) and HDAC6. Tau exhibits intrinsic acetyl-transferase ability, mediated by Cys291 and Cys322 in R2 and R3 repeat, respectively. During auto-acetylation, the most common targets are lysine residues 259, 290, 321 and 353. Acetylation of these sites seems to protect tau from abnormal hyperphosphorylation and is reduced in pathological conditions. Plus, acetylation probably facilitates the fragmentation of tau and enhances its degradation by autophagy. Yet, acetylation on different lysine residues was observed in neurodegenerative diseases. (Alquezar *et al.*, 2021)

Other PMTs mentioned, like glycation, nitration, SUMOylation deamination and others, were observed in tau pathologies, in which they contributed to the disease, except for O-glycosylation, more precisely O-GlcNAc-ylation (addition of N-acetylglucosamine), where this process competes for binding sites of serine/threonine kinases, thus reducing the possibility of hyperphosphorylation and pathology development (Chu and Liu, 2022; Mietelska-Porowska *et al.*, 2014).

3.2 Pathology of tau, tauopathies

Under physiological conditions, tau is a soluble and intrinsically disordered protein. This – among its proper functions – is influenced by PTMs, especially phosphorylation. However, in pathology, tau can undergo hyperphosphorylation, which causes its detachment from microtubules, destabilizing them and impairing axonal microtubular trafficking, and neuronal functions and, consequently, affecting brain functions (Fan *et al.*, 2020)

Furthermore, hyperphosphorylated tau molecules can interact to form paired helical filaments (PHFs) and straight filaments, which subsequently form neurotoxic intraneuronal neurofibrillary tangles (NFTs), a histopathological hallmark of AD. NFTs can potentially reduce the number of synapses, therefore impairing the nervous system further (Goedert, 2020).

In addition, hyperphosphorylated tau aggregates have shown the ability to spread between cells and behave in a prion-like manner, seeding the aggregation of native tau in otherwise

healthy cells. These pathological abilities of tau progressively result in neurodegenerative disorders, commonly called tauopathies (Goedert, 2020).

3.2.1 Tau mutations

Even though there are 112 mutations in the human *MAPT* gene, not all these are pathogenic. Thirteen of these mutations are in an intron, and at least 27 are benign mutations without clinical symptoms. The remaining mutations correlate with neurodegenerative diseases. Fifty-five mutations are found in frontotemporal dementia (FTD) and 15 in AD (most of them are benign). Other are correlated to progressive supranuclear palsy (PSP), Parkinson's disease (PD), Pick's disease (PiD), corticobasal degeneration (CBD) or argyrophilic grain disease. Mutations in exon 10 can alter splicing occurrence, causing an imbalance in 3R/4R isoform levels (Chu and Liu, 2022; Goedert, 2020). However, the altered ratio of tau is not evident in all neurodegenerative diseases. For example, this ratio is still 1:1 in AD. Nonetheless, AD is considered a secondary tauopathy, whereas, in primary tauopathies, the 3R/4R ratio is altered (Table 1) (Fuster-Matanzo *et al.*, 2018). Many *MAPT* mutations are used in different experimental models of tauopathy, such as P301L, P301S and P301T mutations, which are present in behavioural-variant FTD (Goedert, 2020)

Despite two *MAPT* haplotypes – H1 and H2, their connection to disease remains unclear (Chu and Liu, 2022). On the other hand, the H1 haplotype is considered a risk factor for PSP and CBD but not for PiD (Goedert, 2020)

Table 1: Examples of 3R/4R tau ratios in different tauopathies (according to Fuster-Matanzo *et al.*, 2018).

Tauopathy	3R/4R tau ratio
Pick's disease	3:1
Frontotemporal dementia with parkinsonism-17	1:2
Argyrophilic grain disease	1:2
Corticobasal degeneration	1:2
Progressive supranuclear palsy	1:3-4
Parkinson-dementia complex	1:1
Alzheimer's disease*	1:1

* - secondary tauopathy

3.2.2 Abnormal posttranslational modifications

The prime suspect of tau pathology is usually hyperphosphorylation – the excess addition of phosphate residues. However, recently, other PTMs have also attracted attention asa possible cause of pathology (Alquezar *et al.*, 2021)

In the longest human tau isoform (2N4R tau), there are 85 phosphorylation sites (44 serine, 35 threonine and 5 tyrosine residues), which make up almost 20 % of tau to be possibly phosphorylated. Forty-four residues were abnormally phosphorylated in tauopathy patients, mainly in MBD or proline-rich domain. Phosphorylation outside these domains does not damage the ability to bind microtubules but may contribute to aggregation potential. Some of these residues, however, are phosphorylated in the normal healthy brain with ageing (Alquezar *et al.*, 2021; Chu and Liu, 2022), which may indicate that they contribute to pathology but do not cause it *per se*. Many phosphorylated sites are part of degradation signalling motifs.

Nevertheless, in tauopathies, tau degradation is retarded; therefore, the already phosphorylated tau can accumulate in the cell and be subject to further (hyper)phosphorylation. A heterogeneity in phosphorylated sites in soluble, oligomeric PHFs, NFTs and seeding-competent aggregates is observed among the patients afflicted with tauopathy (as reviewed by Chu and Liu, 2022). But certain hotspots are present, for example, phosphorylation at Thr181, Th217, Thr231/Ser235, and Ser262. Phosphorylations at Ser235 and Ser262 residues correlate with the seeding activity of tau aggregates. Overexpressed and overactivated kinases also cause hyperphosphorylation of tau. Interestingly, dephosphorylation of p-tau by PP2A, even species of tau in AD, can restore its microtubule assembly activity and diminish propagation of p-tau in mouse AD models. However, in disease conditions, the enzymatic activity of PP2A is reduced in half; therefore, its rescue abilities are diminished, and the possibility of hyperphosphorylation is increased (Chu and Liu, 2022).

According to Alquezar *et al.* (2021), acetylation of tau may challenge the position of phosphorylation as the key PTM, first recognized in connection to tauopathy in mouse models and later in brain lysates of early-stage AD patients. 2N4R tau isoform incorporates 44 lysine residues, which makes 10 % of tau available for acetylation. The effect of tau acetylase CBP appears to be different in distinct tauopathies. In frontotemporal lobar dementia (FTLD), the CBP activity was found to be increased,

whereas, it was decreased in the frontal cortex and hippocampus in AD patients. Concurrently, deacetylation by Sirt1 and HDAC6 have a different effect as well, whereas, *in vitro*, deacetylation by Sirt1 has a protective role against the accumulation of tau. HDAC6 seemingly contributes to further tau phosphorylation and aggregation. The effect of acetylation, like in phosphorylation, seems to be site-specific, where acetylation of Lys280 weakens the binding of tau to the microtubule, and acetylation of Lys 259, 290, 321 or 353 suppresses further phosphorylation and aggregation. These four sites are commonly acetylated in the healthy brain, whereas in disease, acetylation at these sites is reduced (Alquezar *et al.*, 2021; Goedert, 2020)

Furthermore, acetylation sites are also common sites of other PTMs, such as ubiquitination, SUMOylation, glycation or methylation. Thus, acetylation may serve as a competitive process for other PTMs, either in positive conferring protection from neurodegeneration or negative promoting pathology. For example, ubiquitination of lysine residues makes tau susceptible to degradation via one of the possible degradation pathways – proteasome pathway and autophagy-lysosomal pathway (Alquezar *et al.*, 2021). Ubiquitin residues were found in tau aggregates in AD patients; however, its contribution to the pathology remains unclear, with the possibility of being tagged to tau after the NFT formation (Alquezar *et al.*, 2021). Similarly, the effect of SUMOylation remains to be elucidated; however, recent findings suggest that it may prevent ubiquitination of tau and promote tau degradation by autophagy (Alquezar *et al.*, 2021) On the contrary, other findings, reviewed by Chu and Liu (2022), suggest that it may be the opposite - SUMOylation preventing degradation and promoting phosphor-tau accumulation, based on colocalization of SUMOylation and hyperphosphorylation in AD brains.

3.2.3 Impaired degradation

There are two pathways for tau protein degradation – the ubiquitin-proteasome (UPS) and autophagy-lysosomal pathways. In neurodegeneration, tau degradation is often debilitated, thus allowing hyperphosphorylated tau accumulation and aggregation.

In AD, proteasomal activity (especially trypsin-like activity of 20S particle of proteasome) is disturbed. Endogenous monomeric – either full length or truncated – tau ubiquitinylated by CHIP (C-terminus of Hsc70-interacting protein) is degraded in proteasomes and natively unfolded tau can be degraded by 20S particle even without ubiquitination (Alquezar *et al.*, 2021, David *et al.*, 2002, Lee *et al.*, 2013)

Nonetheless, proteasomes cannot degrade hyperphosphorylated PHFs, even after ubiquitination, and their function is disturbed (Alquezar *et al.*, 2021; Hamano *et al.*, 2021, Poppek *et al.*, 2006). Other PTMs also affect UPS degradation, such as phosphorylation of proline-directed serine-threonine site of tau leads to selective ubiquitination by CHIP and phosphorylation in KXGS motifs, which prevents ubiquitination. Also, six sequences in tau serve as phosphodegrons, meaning that after the phosphorylation of these sites, tau is targeted for degradation. A152T variant of tau has increased phosphorylation of Thr153, preventing the recognition of phosphodegron near the site. Interestingly,proteasome subunits and ubiquitin-ligases colocalize with tau aggregates in AD brains (Alquezar *et al.*, 2021, Lee *et al.*, 2013).

Autophagy-lysosomal pathway (reviewed in more detail in Hrubý, 2020) uses membranous organelles to digest defective parts of cells – organelles, molecules, or parts of cytoplasm with its contents. Three main types of autophagy exist– macroautophagy (commonly called autophagy), microautophagy and chaperone-mediated autophagy. Tau is degraded by macro- and chaperone-mediated autophagy, depending on its number of N-terminal repeats. However, in tauopathies, autophagy can be hindered, possibly by saturation by defective tau aggregates, and the presence of the other stressors can lead to the exhaustion of proteolytic systems and, progressively, cell death and neurodegeneration. Autophagy is, therefore, one of the targets in research on tauopathy treatment (Hrubý, 2020). Whether a faulty tau degradation process is the root of the accumulation of aberrant tau species leading to neurodegeneration or the presence of PHFs and NFTs debilitates proteolytic processes remains to be elucidated (Alquezar *et al.*, 2021).

3.2.4 Tau aggregates formation and propagation

Under pathological conditions, tau cannot bind to the microtubule, most commonly due to its PTMs or *MAPT* gene mutations, and accumulate in cells due to debilitated clearance mechanisms. Accumulated monomeric hyperphosphorylated tau can create oligomeric filamentous structures – PHFs that develop into NFTs. Furthermore, misfolded tau exhibits prion-like properties, which can recruit other non-misfolded molecules into amyloid structures. Apart from tau, other proteins, such as amyloid precursor protein (APP) or α-synuclein, can also serve as protopathic seeds required for amyloid formation and neurodegeneration. These prion-like proteins can transfer cell-to-cell and across nervous systems, but, fortunately, no transmission between two separate organisms was

not observed, unlike in prion diseases (Chu and Liu, 2022; Mirbaha *et al.*, 2018). Tau aggregation can also be triggered *in vitro* by aggregation inducers like heparin (Ye *et al.*, 2022; Zeng *et al.*, 2021).

The inner structure of tau aggregates is not easy to characterize due to the disordered nature of the protein and the existence of many isoforms (Ye *et al.*, 2022; Zeng *et al.*, 2021). However, the core of aggregate (PHF or NFT) is made of MBDs of monomers, especially from the second half of R1 to the first half of R4 repeat – this range may depend on the type of tauopathy. For example, in AD, the core is made only of the regions of R3 and R4. Prominent suspects of aggregation ability are PHF6* and PHF6 motifs (Chu and Liu, 2022; Mirbaha *et al.*, 2018; Ye *et al.*, 2022; Zeng *et al.*, 2021). The presence of MBDs in the core is due to its structure and ability to form β-sheet structures in otherwise highly disordered proteins, thus facilitating the addition of other tau monomers to the group. The rest of the tau molecules are mobile and projecting away, creating a fuzzy coat (Ye *et al.*, 2022; Zeng *et al.*, 2021). The study by Mirbaha *et al.* (2018) observed two distinct monomeric tau species obtained from fibrils after sonication, dubbed "Mi" (inert) and "Ms" (seeding-competent). Conformation modelling of said monomers revealed differences in MBD. In Mi, PHF6 and PH6* motifs were hidden, but in Ms, the motifs were exposed, and other methods supported this model. Ms monomers were found in both *in vitro*-prepared and AD brain tangles. PTMs and tau mutations can also remodel the conformation of tau monomers, thus promoting aggregation. For example, ΔK280 mutant tau was found to stabilize β-sheet conformation required for aggregation, and P301 mutants were found to alter the metastable structure of the PHF6 motif and trigger aggregation, while other mutations in hexapeptide motifs were found to weaken it (Zeng *et al.*, 2021). Mimics of phosphorylation reduced electrostatic interaction between N-terminal and proline-rich domains and moved N-terminal domains away from C-terminal domains, thus making the conformation different from inert tau and enhancing the aggregation ability (Zeng *et al.*, 2021).

Soluble tau oligomers have been suggested as the toxic tau species *in vivo*, capable of intercellular transfer, neurotoxicity, and neurodegeneration (Ye *et al.*, 2022; Zeng *et al.*, 2021). Tau in such oligomers may be different in conformation to monomeric tau species, based on no reactivity of tau monomer antibodies. Oligomers can convert to amyloid fibrils, possibly by exposing MBD upon oligomerization. (Zeng *et al.*, 2021).

As different diseases have different compositions of tau isomers, the conformation of tau filaments in these diseases can be different. In AD, PHFs and straight filaments were found, with both having similar C-shape (Fig. 3A), and the core was made of R3 and R4 and part of the C-terminal domain – R' repeat. In PiD, different filaments were found, narrow and wide, made of a single protofilament and two narrow filaments. In PiD, the core is more elongated than in AD, and is made of 3R tau (Fig. 3C). In CBD, the filament core is entirely different from the other mentioned diseases (Fig. 3B) and is made of 4R tau. Interestingly, these conformations were similar when isolated from patients with the same disease (Oakley *et al.*, 2020; Zeng *et al.*, 2021).

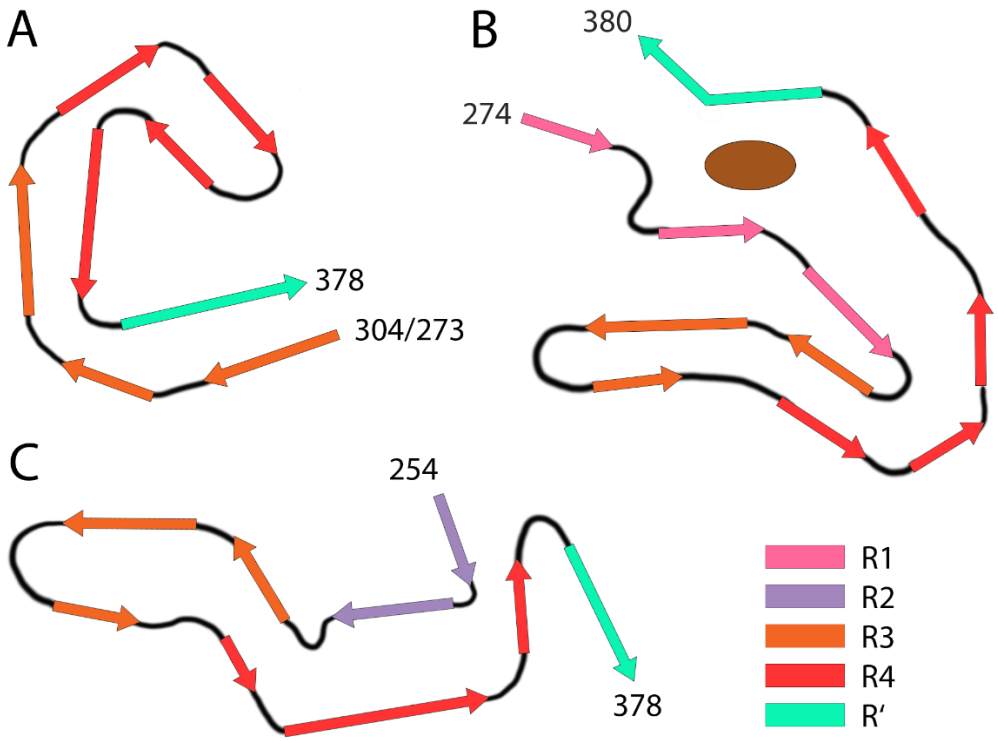

Figure 3: Distinct tau filaments in disease: A - C-shaped 3R/4R filament in AD; B - 4R filament found in CBD. Brown spot - uncharacterized density; C - elongated 3C filament in PiD (according to Zeng *et al.*, 2021)

Tau can be secreted into extracellular space both in physiological and pathological conditions and was found in cerebrospinal fluid and blood of AD patients (Liang *et al.*, 2022). P-tau in cerebrospinal fluid is also used as a marker in suspected AD patients, among amyloid-β and total tau. Total tau serves as a marker of cellular death and cytoskeletal disruption and is not specific to AD, unlike amyloid-β, which forms plaques in AD brain tissues (Koudelková, 2009).

4 MATERIALS AND METHODS

4.1 Cell line

- Tau RD P301S FRET Biosensor cells (ATCC® CRL-3275™)

4.2 Equipment and software

Equipment:

- Automatic pipetting filler Pipetus® (Hirschmann, Germany)
- Cell Voyager CV7000S (Yokogawa, Japan)
- CellCarrier-96 Microplates (PerkinElmer, USA)
- Centrifuge 5810R (Eppendorf, Germany)
- ChemiDoc MP analyser (BioRad, USA)
- Electrophoresis and Blotting Vertical Apparatus (BioRad, USA)
- HeracellTM VIOS incubator (ThermoFisher Scientific, USA)
- MSC-Advantage Biological Safety Cabinet (flow-box) (Thermo Fisher Scientific, USA)
- Rotina 420 R Centrifuge (Hettich Zentrifugen) (Hettich, Germany)
- ViCell XR Cell Viability Analyzer (Beckman Coulter Inc., USA)
- Vortex V-1 Plus (Biosan, Latvia)

Software:

- ImageJ, ver. 1.53q
- Prism 8 (GraphPad, USA)
- Microsoft Excel, ver. 2206
- Columbus Image Data Storage and Analysis System, ver. 2.7

4.3 Chemicals and solutions

Chemicals:

- 10x Tris/Glycine/SDS (Bio-Rad, #1610772]
- 30% Acrylamide/Bis-acrylamide 29:1 (Bio-Rad, #1610156)
- Bovine serum albumin (BSA) (Sigma-Aldrich, #A2153)
- Dulbecco's Modified Eagle Medium (Lonza, #12-604F)
- Hoechst-33342 nuclear dye (Invitrogen, #H21492)
- jetPRIME® polyplus transfection kit (Polyplus infection, #114-15)

- PhosSTOP™ (Roche, #04906845001)
- Protease Inhibitor Cocktail Tablets (Roche, #04693116001)
- Resolving gel buffer 1.5 M Tris-HCl pH 8.8 (Bio-Rad, #161-0798)
- Spectra™ Multicolor Broad Range Protein Ladder (Thermo Fisher Scientific, #26634)
- Stacking gel buffer 0.5 M Tris-HCl pH 6.8 (Bio-Rad, #161-0799)
- Tetramethylethylenediamine (TEMED) (Bio-Rad, #1610801)
- TrypLE™ Express Enzyme (1X), no phenol red (Thermo Fisher Scientific, #12604013)

Stock solutions:

- 10x PBS: 80 g NaCl, 2.0 g KCl, 14.4 g Na_2HPO_4, 2.4 g KH_2PO_4 dissolved in 800 ml dH_2O, pH adjusted to 7.4 with HCl and added dH_2O to 1000 ml, sterilized by autoclaving.
- 10x TBS buffer: 24 g Tris base and 88 g NaCl dissolved in 900 ml dH_2O, pH adjusted to 7.6 with HCl and added dH_2O to 1 000 ml.
- TBST buffer: 1x TBS buffer with 0.1% Tween 20.
- RIPA buffer (radioimmunoprecipitation assay buffer): 150 mM sodium chloride, 1.0% NP-40, 0.5% sodium deoxycholate, 0.1% SDS (sodium dodecyl sulfate), 50 mM Tris, pH 8.0.
- 5× SDS loading buffer: 250 mM Tris-HCl (pH=6.8), 10% SDS, 30% glycerol, 0.5 M DTT, 0.02% bromophenol blue, 10% mercaptoethanol.
- 0.05% Triton X-100 solution (10 mL): 1X TBS with 5 µL Triton X-100.
- 10% (w/v) SDS.
- 5% (w/v) BSA blocking solution: 2.5 g BSA dissolved in 40 ml of TBST buffer, added TBST to 50 ml.
- 10% resolving polyacrylamide gel (10 mL): 3.8 ml dH_2O, 3.4 ml 30% acrylamide/bis-acrylamide, 2.6 ml resolving gel buffer, 100 µl 10% (w/v) SDS, 100 µl 10% (w/v) APS, 10 µl TEMED.
- Stacking polyacrylamide gel (5 mL): 2.975 ml dH_2O, 670 µl 30% acrylamide/bis-acrylamide, 1.25 ml stacking gel buffer, 50 µl 10% (w/v) SDS, 50 µl 10% (w/v) APS, 5 µl TEMED.

4.4 Antibodies

- Donkey anti-Mouse IgG (H+L) Highly Cross-Adsorbed Secondary Antibody, Alexa Fluor 488 (Thermo Fisher Scientific, #A-21202), 1:2000
- Goat anti-Rabbit IgG (H+L) Highly Cross-Adsorbed Secondary Antibody, Alexa Fluor 488 (Thermo Fisher Scientific, #A-11034), 1:2000
- Mouse anti-GAPDH Monoclonal Antibody (Santa Cruz Biotechnology, #sc-32233), 1:4000
- Mouse anti-Tau5 Monoclonal Antibody (Thermo Fisher Scientific, #AHB0042), 1:1000
- Rabbit anti-Phospho-Tau (Ser262) Polyclonal Antibody (Thermo Fisher Scientific, #OPA1-03142), 1:1000

4.5 Methods

Cell culturing

Tau RD P301S biosensor cells were cultivated in complete Dulbecco's modified Eagle's growth medium, supplemented with 10% fetal bovine serum and 1% antibiotics (streptomycin and penicillin), and kept in a humidified incubator with 5 % CO_2 at 37 °C. Cells were passaged every 2-3 days when confluent. Cells were washed with 1× PBS and treated with TrypLE to facilitate detachment. TrypLE was inactivated by adding a complete growth medium. The cell suspension was centrifuged at 300 × g for 5 minutes. Sedimented cells were resuspended in a complete growth medium, and cell number and viability were assessed using Vi CELL XR Cell Counter (Beckman Coulter).

Seeding Tau P301S biosensor cells with Tau R2 and R3 aggregates by transfection

For fluorescent microscopy analysis, cells were plated on CellCarrier 96-well plate (5×10^4 cells/mL, 100 µL of medium/well) and kept in a 5% CO_2 incubator at 37 °C overnight. The transfection mixture was prepared using a jetPRIME® Polyplus transfection kit. An 18-step two-fold serial dilution of R2 and R3 aggregates in jetPRIME® buffer (5 µL/well) was prepared, starting with 100 nM of tau in a total volume of 100 µL of growth media/well. Tau aggregates were mixed with jetPRIME® buffer. After serial dilution, jetPRIME® reagent (0.5 µL/well) was added, and mixtures were briefly vortexed and incubated for 10 minutes at room temperature. During incubation, the medium in theassay wells was changed to a fresh one. After incubation, a respective volume was added to the growth medium in wells. jetPRIME® buffer and reagent without aggregates were used as a control sample. The cells were then incubated at 5% CO_2/37 °C for 3, 24, 48 and 72 hours.

For western blot analysis, cells were plated on 10cm Petri dishes ($1{,}5 \times 10^6$ cell/dish, 10 mL medium/dish) and kept in a 5% CO_2 incubator at 37 °C overnight. The transfection mixture was prepared using a jetPRIME® Polyplus transfection kit. A 16-step two-fold serial dilution of R2 or R3 aggregates was prepared, starting with 100 nM concentration of aggregates (in a total volume of 10 mL of growth medium per culture dish). Tau aggregates were mixed with jetPRIME® buffer (500 µl/well) and serially diluted in the respective volume of jetPRIME® buffer. After serial dilution, every third concentration (1^{st}, 4^{th}, 7^{th}…16^{th}) was selected for further steps. jetPRIME® reagent (10 µL/tube) was added, and mixtures were briefly vortexed and incubated for 10 minutes

at room temperature. During incubation, the medium in the dishes was changed to a fresh one. After incubation, a respective volume was added to the growth medium in the dishes. jetPRIME® buffer and reagent without aggregates were used for a control sample. The cells were incubated in 5% CO_2 at 37 °C for 72 hours.

Fluorescent microscopy and image analysis

Imaging was performed using Cell Voyager CV7000S (Yokogawa) with 60× objective at 37 °C and 5% CO_2 in a live-cell chamber (Annadurai *et al.*, 2022). For the time-dependent tau seeding experiment, cells were imaged every 3 hours for 24 hours after transfection and then after 48 h and 72 h after transfection. For aggregate quantification, cells were imaged at 24, 48 and 72 hours after transfection. Before imaging, nuclei were stained by 10 μM Hoechst 33342 – medium was changed for Hoechst/medium solution and plates were incubated for 10 minutes. After incubation, the medium with dye was changed for a fresh complete medium and cells were imaged. Images were analyzed by Columbus Image Data Storage and Analysis System (Parkin Elmer), and data were processed in Microsoft Excel and GraphPad Prism software.

Western blot sample collection

When collecting samples from 10cm Petri dishes, the growth medium was collected in a conical centrifuge tube. Cells were washed with 1x TBS, and the buffer was collected in the same tube. Cells were treated with 2 ml of TrypLE to facilitate detachment. After detaching, TrypLE was inactivated by the growth medium, and the cell suspension was collected in the tube. Cells were then centrifuged at 300 × g for 5 minutes. After centrifugation, the supernatant was discarded, and sedimented cells were resuspended in 1 ml of 1x TBS, transferred into a 1.5 mL tube and centrifuged at 4 000 RPM for 5 minutes. The supernatant was discarded, and pelleted samples were further processed or stored in a –80 °C freezer.

Sample processing

During all the further steps, samples were kept on ice. Lysis buffer (1x TBS with .0.05 % Triton X-100) was mixed with protease and phosphatase inhibitors. 500 μL of complete lysis buffer was added to pellets. Cells were resuspended by pipetting, and the mixture was incubated for 5 minutes on ice. After the lysis, samples were centrifuged at 500 × g and 1000 × g successively for 5 minutes at 4 °C. Supernatant was transferred into a new tube and was further centrifuged at 15 000 RPM at 4 °C for 60 minutes,

the pellet was discarded. After centrifugation, supernatant with Triton-soluble protein fraction was collected, and the pellet was washed with Triton lysis buffer twice and centrifuged at 15 000 RPM at 4°C for 1 minute after each wash. After washing, the pellet was resuspended in 50 μL of RIPA buffer with inhibitors and sonicated for 1 minute in a water bath sonicator at 50 % amplitude, 15-sec pulse on and 15-sec pulse off. After sonication, tubes were centrifuged at 15 000 RPM at 4 °C for 30 minutes. Supernatant with Triton-insoluble fraction was collected into new tubes, and both fractions were further processed or stored in a –80 °C freezer.

SDS-PAGE Electrophoresis and Western blotting

SDS-polyacrylamide gels (1.5 mm thick, 10%) with 15 wells were hand-cast using Bio-Rad Mini PROTEAN Tetra Cell system, using Tris-Glycine-SDS buffer. Equal volumes (16 μL) of Triton-soluble and insoluble fractions were mixed with SDS gel loading dye (4 μL/well) supplemented with 10% β-mercaptoethanol. Mixtures were heated at 95 °C for 5 minutes in a dry thermal block. After heating and letting it cool down, samples were loaded (20 μL of mixture/well) onto the gels. Electrophoresis was run at 200 V for 1.5 hours until the dye hit the bottom of the gel.

Western blot was done using Trans-Blot Turbo Transfer System – Ready-to-Assemble kit, following the kit's protocol. Proteins were transferred onto a PVDF membrane. A preprogrammed protocol for 1.5mm gel(s) was used for transfer settings, and the transfer time was adjusted to 15 minutes. After blotting, membranes were blocked in 5% BSA in TBS-T solution for 1 hour at room temperature while gently rocked. After blocking, membranes were transferred to 50 mL conical tubes and incubated with primary antibodies anti-Tau5, anti-pSer262 and anti-GAPDH overnight at 4°C on a roller. After incubation, membranes were washed in 1x TBS-T four times in 10 minutes intervals, and the buffer was changed to a fresh one each time. Then, membranes were treated with respective secondary anti-mouse and anti-rabbit antibodies conjugated with Alexa 488 fluorescent dye and incubated for 2 hours at room temperature on a roller. Then, membranes were washed with 1x TBS-T four-times at 10 minutes intervals. After the final wash, membranes were imaged in the Bio-Rad Gel Documentation system, and images were processed using ImageJ software and data analyzed using Microsoft Excel and GraphPad Prism software.

5 RESULTS

5.1 Exogenous R2 and R3 aggregates induced intracellular aggregation with different pSer262/Tau5 ratio

Transfection of Tau-RD-P301S biosensor cells with R2 and R3 fibrils induced the formation of Triton-insoluble tau aggregates, which was confirmed by Western blotting (Fig. 4, 5) and fluorescent microscopy (Fig. 8, 10, 11). The detected pSer262 and Tau5 levels in both Triton-soluble and insoluble fractions were analyzed using ImageJ and Graphpad Prism software. Following R3 aggregate treatment, the pSer262/Tau5 ratio in the Triton-insoluble fraction was observed to be in favour of tau phosphorylated at Ser262 (Fig. 4), whereas after R2 treatment, Triton-insoluble Tau5 levels were visually greater in comparison to insoluble pSer262 levels (Fig. 5A)

5.2 Exogenous R2 and R3 aggregates induce intracellular aggregation with similar potency over time

Induction of intracellular tau aggregation after transfection with R2 and R3 aggregates was observed by imaging on a Cell Voyager CV7000S (Yokogawa), and the acquired images were analyzed using Columbus Image Data Storage and Analysis System (PerkinElmer). For quantification purposes, the numbers of aggregates were detected as spots of P301S/CFP/YFP tau and normalized to the number of cells detected by Hoechst-stained nuclei. EC_{50} value was established as a concentration of aggregates (seeds) needed to induce half of the maximal aggregate/nuclei ratio. Following both R2 and R3 treatments, a decrease in EC_{50} value was observed over time (Fig. 6, 7, 9) as the number of aggregates increased (Fig. 8). The EC_{50} values were 39.57 nM, 14.83 nM and 14.04 nM after 24, 48 and 72 hours, respectively, of treatment with R2 aggregates. Similarly, the EC_{50} values were 30.63 nM, 13.72 nM, and 16.56 nM, respectively, after 24, 48 and 72 hours of treatment with R3 aggregates (Fig. 6, 7). EC_{50} values were visibly different after 24 h incubation, whereas after 48 and 72 h, no significant difference was observed (Fig. 9).

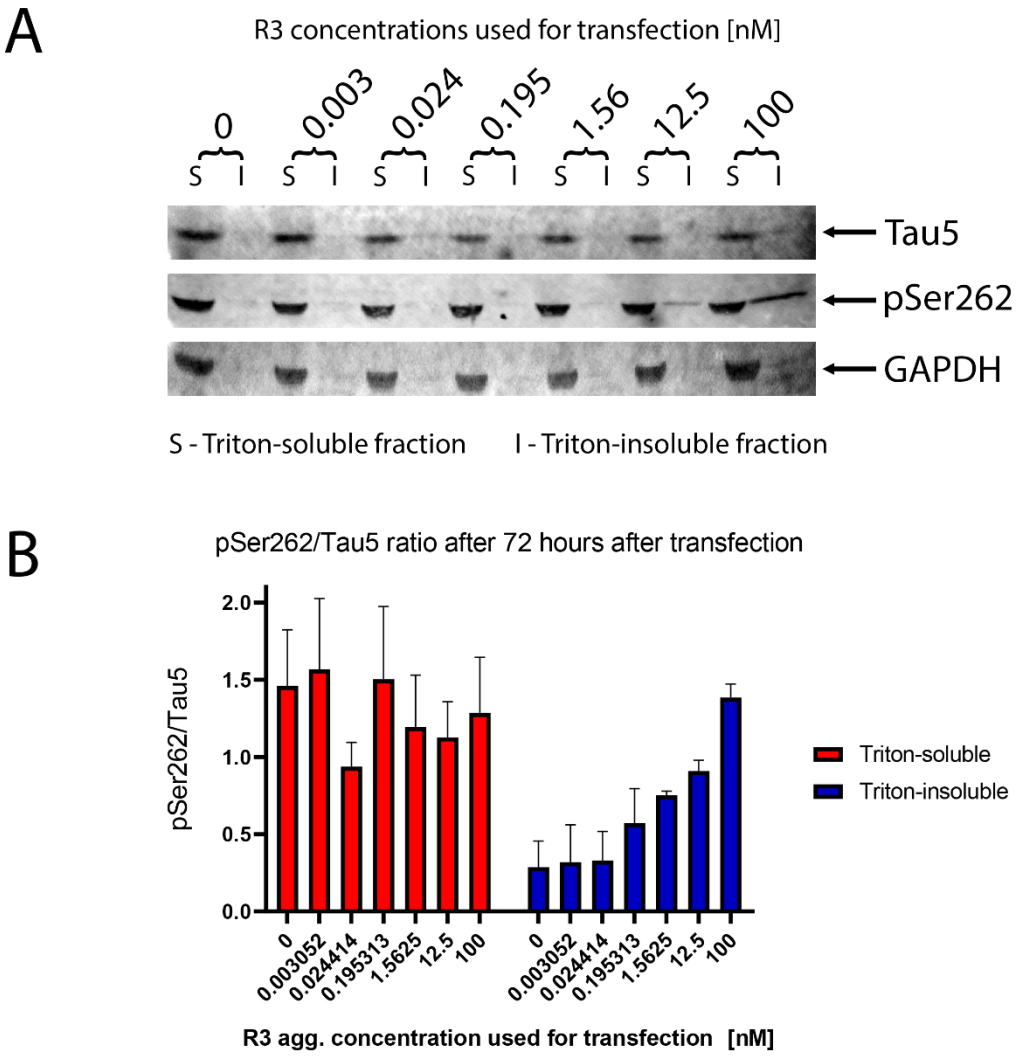

Figure 4: A- Western blot of Tau5, pSer262 and GAPDH in Triton-soluble (S) and Triton-insoluble (I) fractions after 72 hours of treatment with R3 fibrils. B - analysis of ratios of pSer262/Tau5 levels detected by Western blot in Triton-soluble and Triton-insoluble fractions. Data shown are mean ± SEM, n = 3.

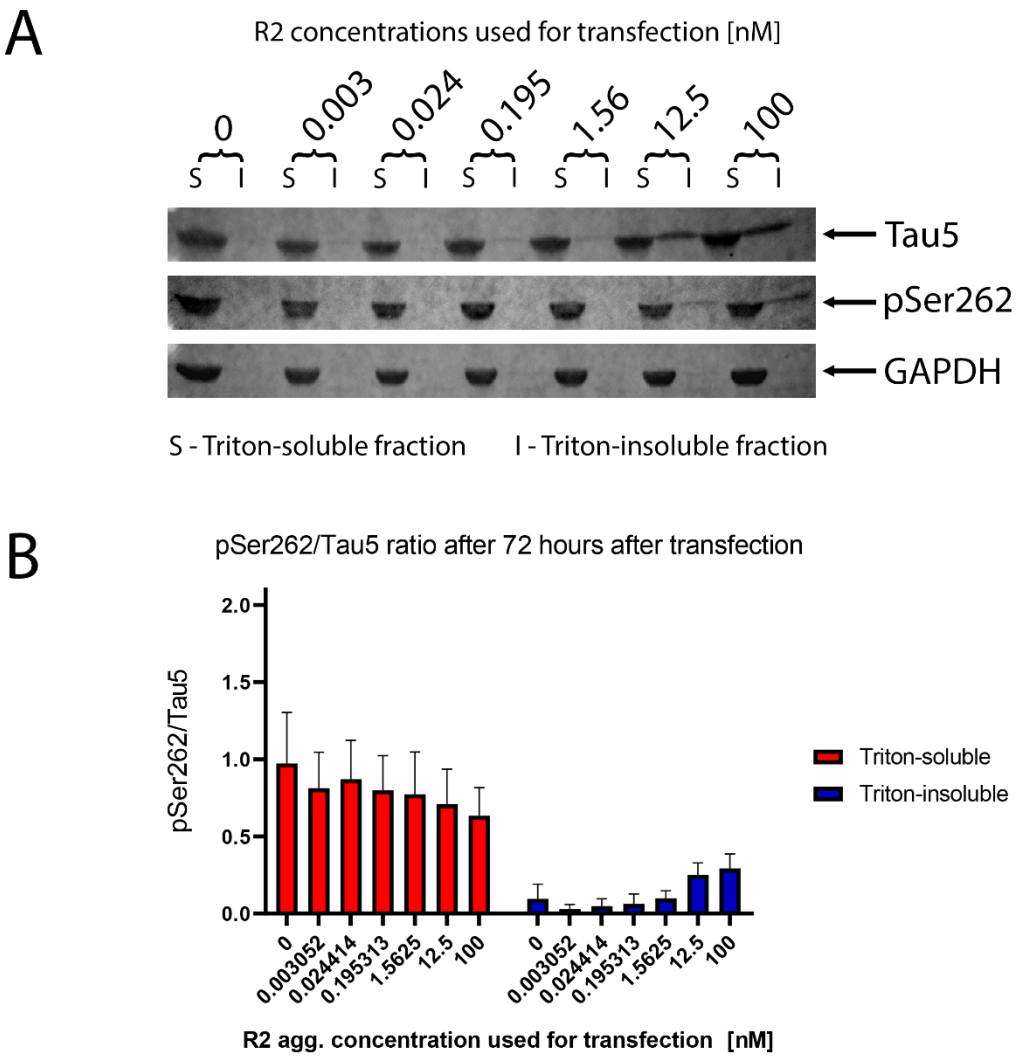

Figure 5*:* A- Western blot of Tau5, pSer262 and GAPDH in Triton-soluble (S) and Triton-insoluble (I) fractions after 72 hours of transfection with R2 fibrils. B - analysis of ratios of pSer262/Tau5 levels detected by Western blot in Triton-soluble and Triton-insoluble fractions. Data shown are mean ± SEM, n = 3.

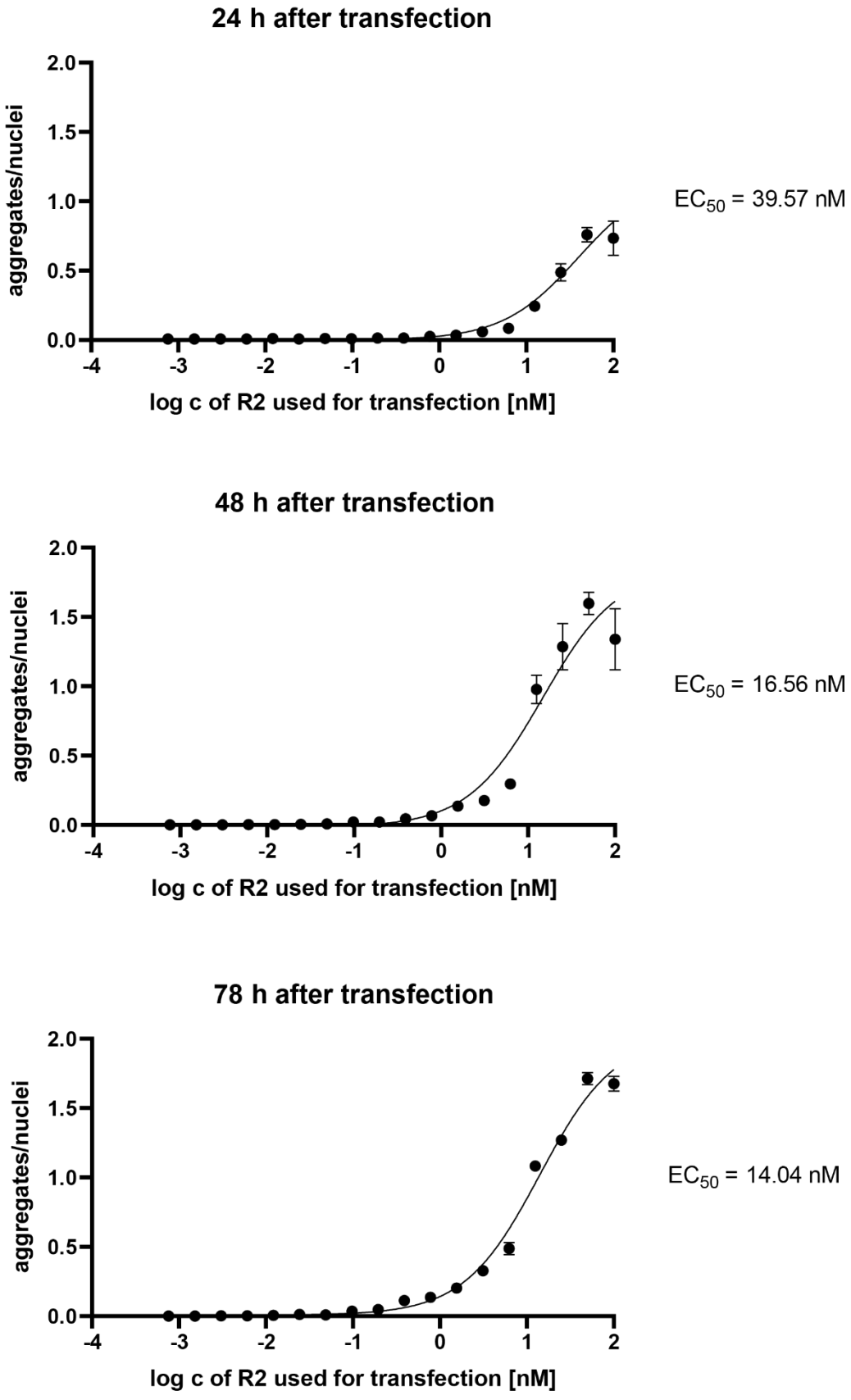

Figure 6: Determination of EC_{50} value of R2 fibrils after 24, 48 and 72 h of transfection. Data shown are mean ± SEM, n=4.

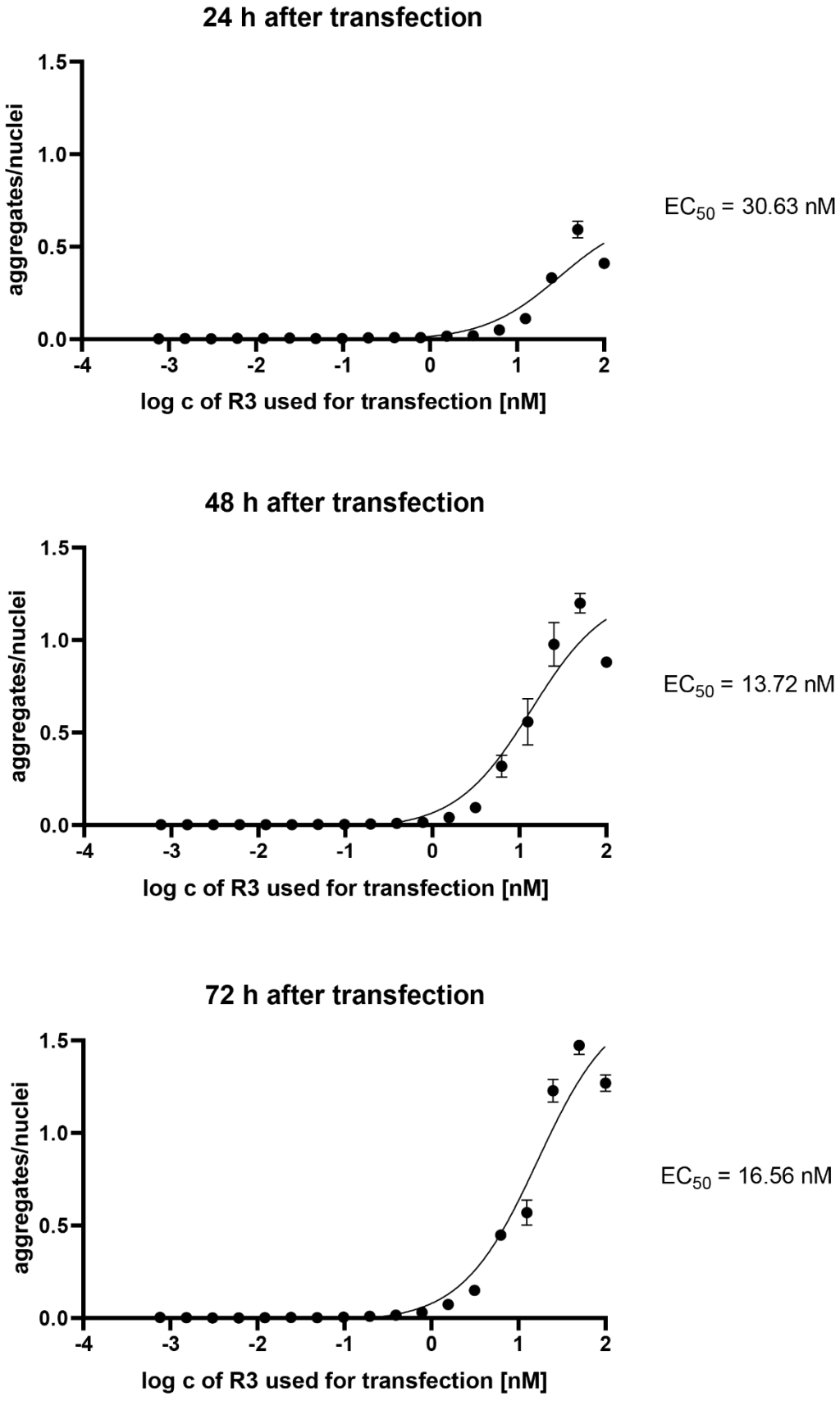

Figure 7: Determination of EC_{50} value of R3 fibrils after 24, 48 and 72 h of transfection. Data shown are mean ± SEM, n=4

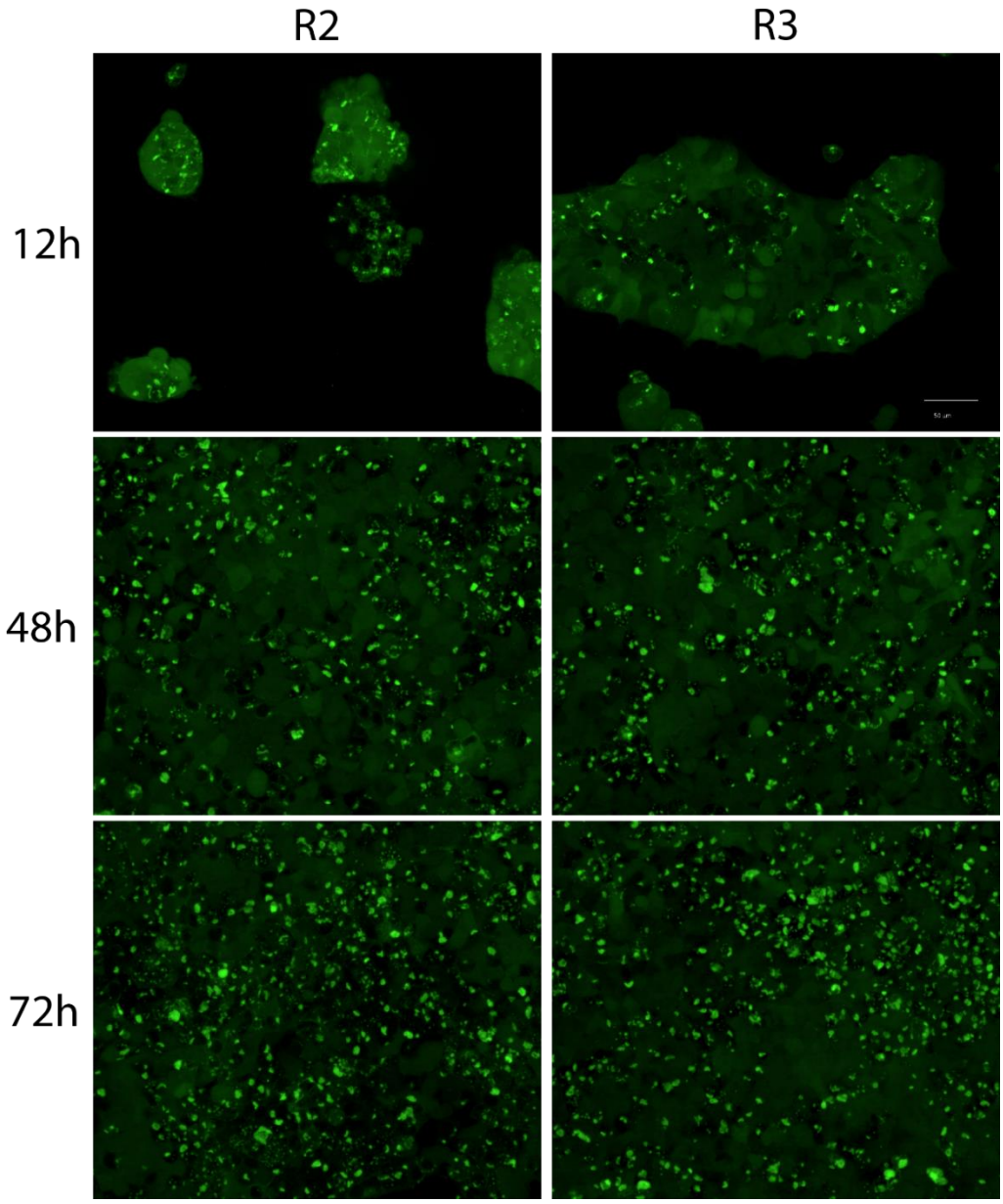

Figure 8: Images showing the time-dependent increase in the induction of intracellular aggregation of native tau (green inclusions) in biosensor cells after transfection with 50 nM fibrils (E_{max}) of R2 and R3.

5.3 Exogenous R2 aggregates induce intracellular aggregation with higher efficacy

Different maximal aggregate/nuclei ratio (E_{max}) was observed after R2 and R3 transfection. In cells treated with R2 fibrils, the maximal aggregates/nuclei ratio was 0.76, 1.60 and 1.71 after 24, 48 and 72 hours, respectively. After R3 fibril treatment, E_{max} was 0.59, 1.20, and 1.47 after 24, 48 and 72 hours, respectively. Therefore, R2 seeds are more efficacious for induction of intracellular aggregate formation (Fig. 6, 7, 9)

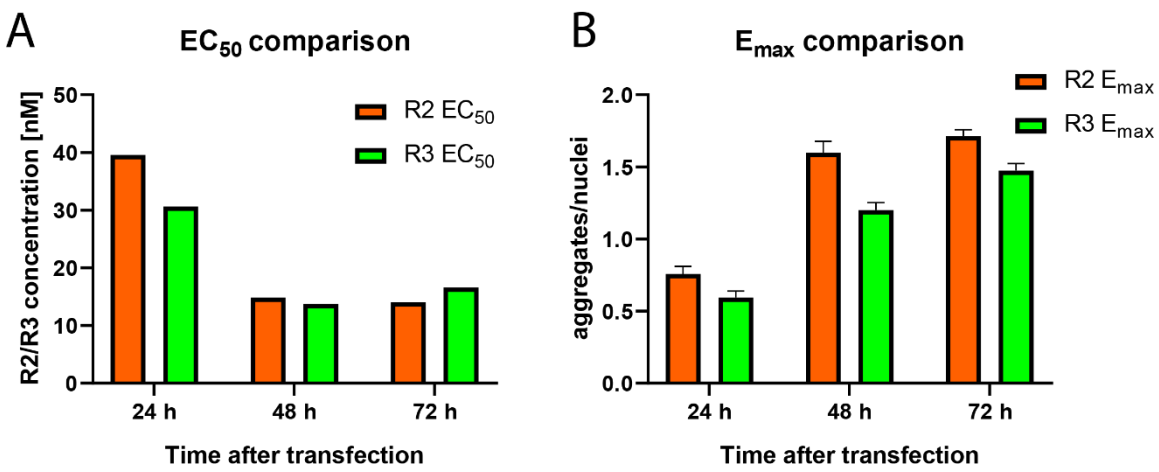

Figure 9: A – Comparison of EC_{50} values of R2 and R3 based on the induction of intracellular tau aggregation, shown in Fig. 6, 7.. B - Comparison of E_{max} values of R2 and R3 fibrils after transfection, data shown as mean ± SEM, n = 4.

5.4 E_{max} is achieved by the same concentration in both R2 and R3

After R2 and R3 treatment, E_{max} was observed by transfecting the Tau-RD-P301S biosensor cells with 50 nM fibrils (Fig. 6, 7, 8). At the higher concentration (100 nM), the aggregates/nuclei ratio decreased since a lower number of aggregates and nuclei were detected (data not shown), suggesting higher toxicity of exogenous aggregates in higher concentrations than 50 nM.

5.5 R2 aggregates induce intracellular aggregation earlier and more rapidly than R3 aggregates

In experiments where the cells were transfected with R2 fibrils and then continuously imaged for 24 h at 3h intervals, intracellular tau aggregation were observed as early as 3 hours following transfection with 100 nM fibrils, whereas intracellular aggregation was observed after 9 hours of R3 fibrils transfection (Fig. 10). I also displayed that in R2 treatment, the number of aggregates increases faster than after R3 treatment. Therefore, R2 fibrils seed intracellular aggregation more efficiently.

Figure 10: Induction of intracellular tau aggregation after transfection with 100 nM fibrils of R2 (A) or R3 (B) for 24 hours. The time after transfection is indicated in the upper left corner. White arrows - first occurring intracellular aggregates

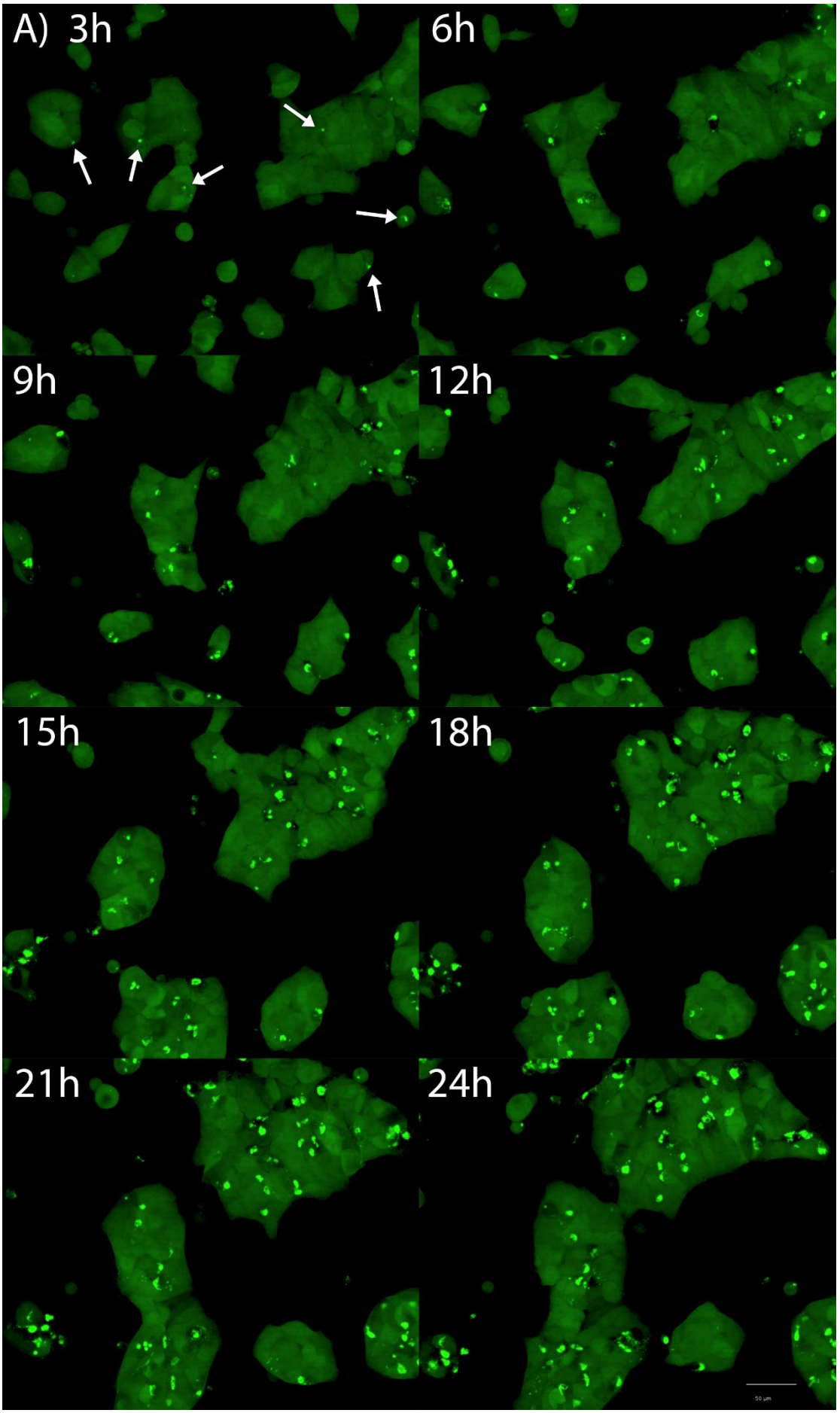
A) 3h
6h
9h
12h
15h
18h
21h
24h

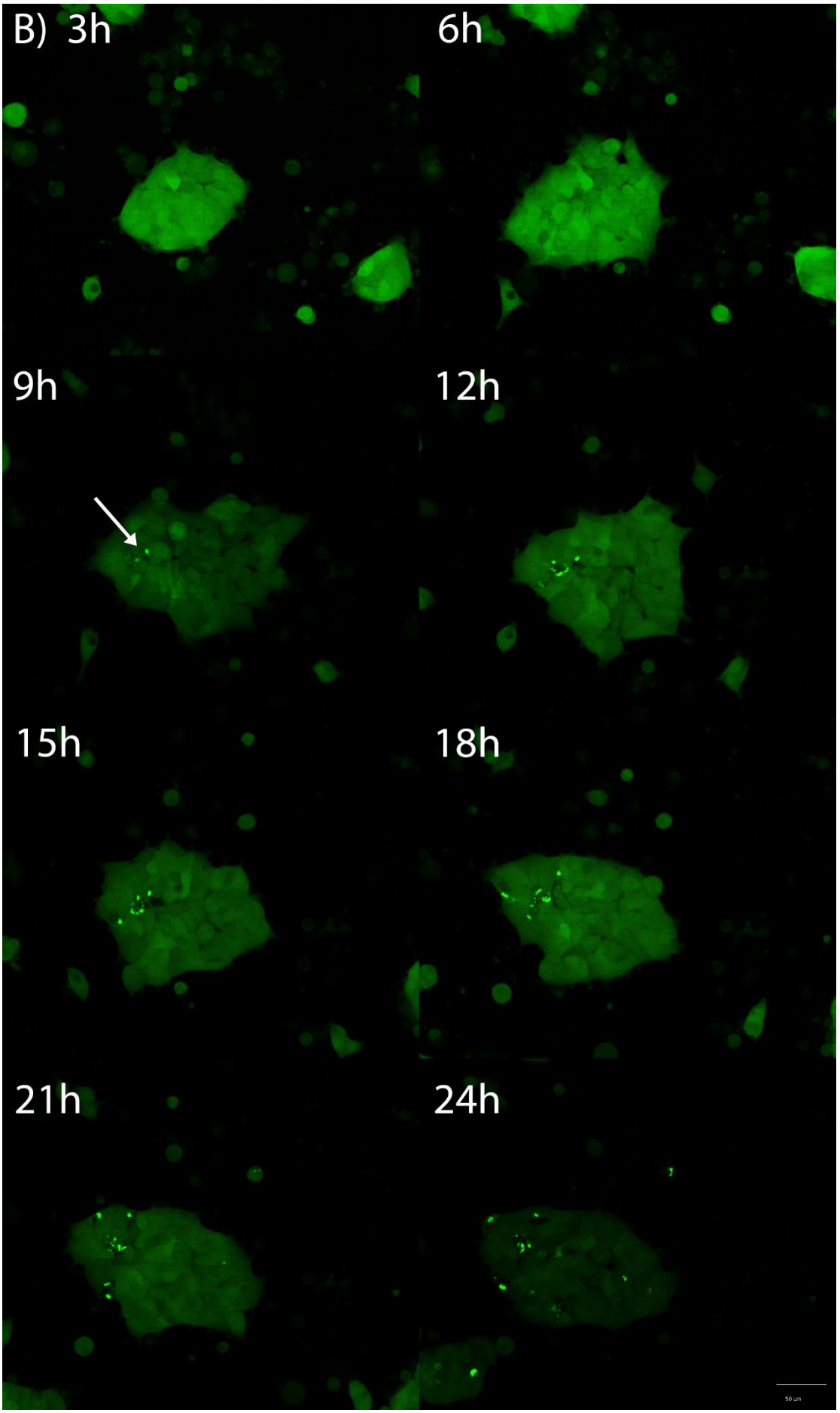
B) 3h
6h
9h
12h
15h
18h
21h
24h
50 µm

5.6 R2 and R3 fibrils show identical minimal concentration needed for seeding

In both treatments, the minimal concentration needed for visible seeding under the microscope was equal in respective time points. After 24, 48 and 72 hours of transfection, the minimal concentration of fibrils was 6.25 nM, 0.006 nM, and 0.001 nM, respectively (Fig. 11).

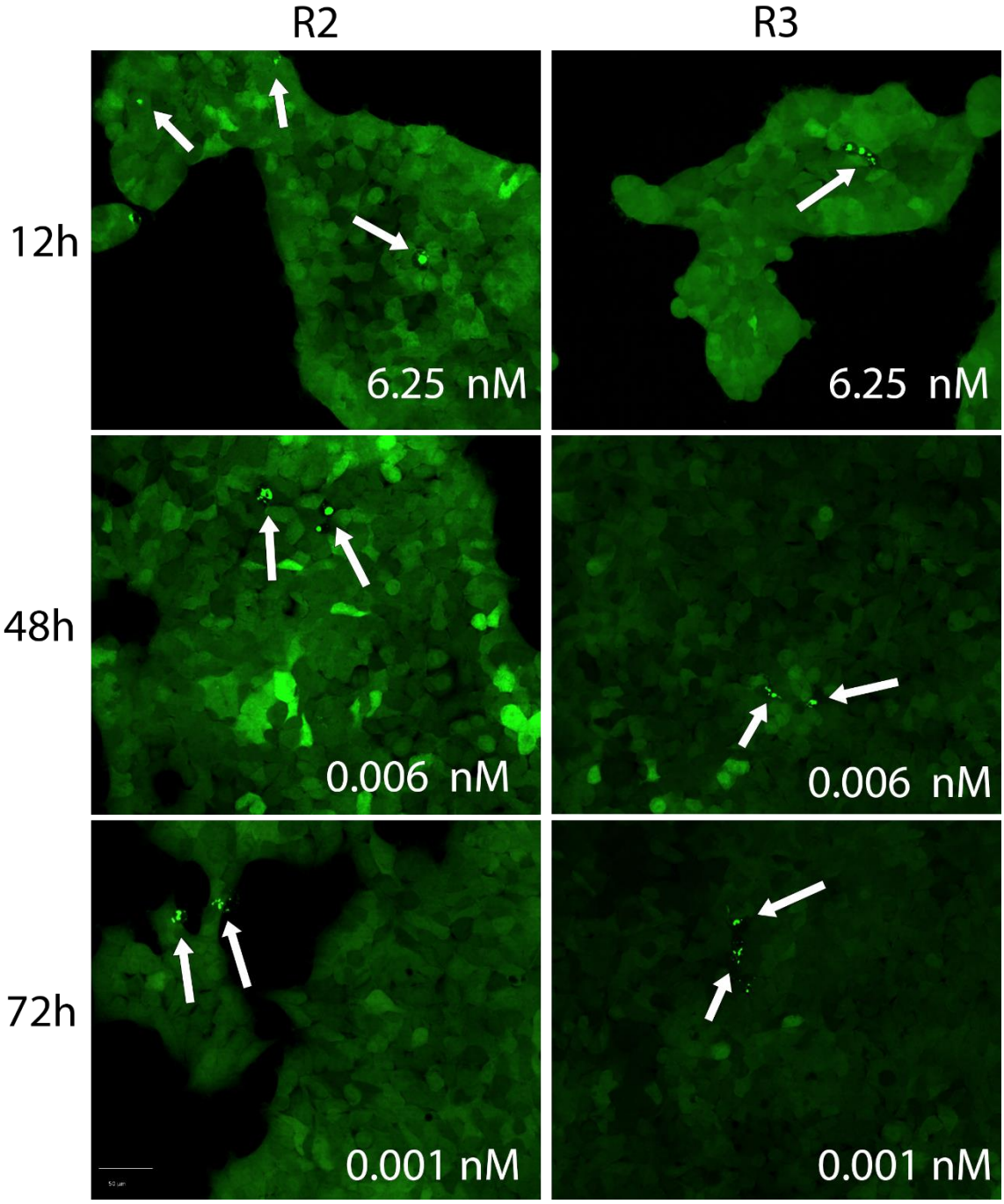

Figure 11: Minimal concentration of exogenous tau fibrils needed for aggregation induction in different timepoints White arrows point to intracellular aggregates.

5.7 Summary of values determined by fluorescent microscopy analysis

Values obtained using fluorescent microscopy analysis are summarized in Table 2.

Table 2: Overview of data obtained using fluorescent microscopy

Type of fibrils		**R2**	**R3**
EC_{50} [nM]	24 hours	39.57	30.63
	48 hours	16.56	13.72
	72 hours	14.04	16.56
E_{max} (aggregates/nuclei)	24 hours	0.76	0.59
	48 hours	1.60	1.20
	72 hours	1.71	1.47
E_{max} concentration [nM]		50	50
Minimal concentration required [nM]	24 hours	6.25	6.25
	48 hours	0.006	0.006
	72 hours	0.001	0.001
Time of first intracellular aggregates appearance post transfection		3h	9h

6 DISCUSSION

Protein aggregates are hallmarks of neurodegenerative diseases. Due to alternative splicing, tau is expressed into 6 isoforms, distinguished by the number of repeats in MBD – 4R and 3R. Both 4R and 3R isoforms contribute to the formation of tau aggregates – PHFs and NFTs in tauopathies. It has been shown (Annadurai *et al.*, 2022a) that hexapeptide motifs - VQIVYK of R3 repeat and VQIINK in R2 repeat - are essential for tau aggregates to form β-sheet structures, thus allowing clustering of hyperphosphorylated tau. It has also been shown (Annadurai *et al.*, 2022a, 2022b; Hrubý, 2020) that exogenous tau R2 and R3 peptide fibrils containing these motifs can induce intracellular tau aggregation, making the hexapeptide motifs pharmacological targets for tau aggregation and seeding/spreading inhibitors (Seidler *et al.*, 2019). However, more detailed comparative studies on induced intracellular aggregation after treatment with R2 and R3 fibrils are needed for future development of tauopathy models, tauopathy treatment and possible diagnostic approaches for tauopathies, which utilize tau biosensor models (Lathuiliere and Hyman, 2021)

Similar to Annadurai *et al.* (2022b), I observed an increased tau (total, Tau5) band intensity in the Triton-insoluble protein fraction after R2 transfection compared to the total tau band intensity after R3 transfection. Therefore, it is possible that seeding with R2 fibrils is responsible for recruiting Triton-soluble oligomers into Triton-insoluble aggregates. Concurrently, I observed a decrease in the phosphorylated/total tau ratio after the R2 treatment. Even though it might suggest a decrease in phosphorylation of tau aggregates, it is possible for tau clusters to recruit unphosphorylated tau for phosphorylation to occur in later stages (Goedert and Spillantini, 2017). Moreover, phosphorylation is not needed for seeding, but seeded aggregates are hyperphosphorylated (Falcon *et al.*, 2015). It is possible that sites other than Ser262 were phosphorylated - Annadurai *et al.* (2022b) suggest other AD-specific phosphorylations, such as Ser394 and Ser404 - which may contribute to hyperphosphorylation. Overall, the findings in this thesis suggest changes in the levels of Triton-soluble and insoluble tau, both total and phosphorylated, depending on the type of fibril used, in concurrence with Annadurai *et al.* (2022b). It would be beneficial to know the differences in PTMs of the aggregates induced by R2 and R3 fibrils, for example, for specific tauopathy models, as some PTMs are more prevalent in certain tauopathies (Kametani *et al.*, 2020)

To compare the effects of R2 and R3 in different conditions, I established the ratio of the number of aggregates detected to the number of nuclei detected, similarly to method used by Annadurai *et al.* (2022a) to eliminate, for example, improper distribution of cells on assay plate wells. EC_{50} values, established as the concentration of tau fibrils required for transfection to induce half of the maximal seeding effect (the highest aggregates/nuclei ratio), decreased over time. Intriguingly, EC_{50} values of R2 and R3 were similar, except in 24-hour incubation, suggesting higher potency of R3 fibrils after 24h treatment. This should be proved by further study. In addition, the minimal concentration needed for seeding was the same in both treatments at distinct time points, and so was the concentration required for the maximal effect of seeding. However, R2 fibrils showed higher efficacy in intracellular aggregation induction, displayed by a higher aggregates/nuclei ratio.

Furthermore, intracellular aggregates were visible six hours earlier after R2 transfection compared to R3 transfection. Interestingly, I observed a decrease in aggregate/nuclei ratio in treatment by 100 nM fibrils, both R2 and R3 fibrils, caused by both decrease in the cell (nuclei) number and the number of aggregates, in comparison to 50 nM treatment, which induced E_{max}. This suggests higher toxicity of fibrils in concentrations higher than 50 nM. It is possible that higher concentrations induce aggregation faster, observed by the earlier occurrence of intracellular aggregates at higher concentrations, creating proteopathic stress that kills the cells earlier, thus lowering the aggregate/nuclei ratio. This should be addressed in further studies, where higher concentrations will be used.

Overall, the findings in this thesis suggest that R2 fibrils are more efficacious and efficient in the induction of intracellular aggregates than R3 fibrils. Further studies should confirm these findings, utilizing flow cytometry as another reliable tau seeding detection method, which could overcome the limitations of fluorescent microscopy (Holmes *et al.*, 2014).

7 CONCLUSION

In this thesis, I compared the differences in the effects of exogenous R2 and R3 fibrils (aggregates) on the induction of intracellular tau aggregation in a FRET biosensor cell line expressing Tau-RD-P301S. I observed that both R2 and R3 aggregates induce the formation of Triton-insoluble tau inclusion with similar potency, and the minimal concentration required for seeding is the same. However, higher efficacy and faster induction of endogenous aggregation were observed in transfection by R2 filaments.

Our findings should shed some light on the differences in the induction of endogenous tau aggregates in the Tau-RD-P301S biosensor cell line after transfection by exogenous R2 and R3 aggregates, hopefully facilitating further research on this topic.

8 REFERENCES

Abubakar, M.B., Sanusi, K.O., Ugusman, A., Mohamed, W., Kamal, H., Ibrahim, N.H., Khoo, C.S., Kumar, J. (2022): Alzheimer's Disease: An Update and Insights Into Pathophysiology. Frontiers in Aging Neuroscience 14: 742408. doi: 10.3389/fnagi.2022.742408.

Alquezar, C., Arya, S., Kao, A.W. (2021): Tau Post-translational Modifications: Dynamic Transformers of Tau Function, Degradation, and Aggregation. Frontiers in Neurology 11: 595532. doi: 10.3389/fneur.2020.595532.

Annadurai, N., Malina, L., Malohlava, J., Hajdúch, M., Das, V. (2022b): Tau R2 and R3 are essential regions for tau aggregation, seeding and propagation. Biochimie 200: 79–86. doi: 10.1016/j.biochi.2022.05.013.

Annadurai, N., Malina, L., Salmona, M., Diomede, L., Bastone, A., Cagnotto, A., Romeo, M., Šrejber, M., Berka, K., Otyepka, M., Hajdúch, M., Das, V. (2022a): Antitumour drugs targeting tau R3 VQIVYK and Cys322 prevent seeding of endogenous tau aggregates by exogenous seeds. The FEBS Journal 289: 1929–1949. doi: 10.1111/febs.16270.

Bakota, L., Ussif, A., Jeserich, G., Brandt, R. (2017): Systemic and network functions of the microtubule-associated protein tau: Implications for tau-based therapies. Molecular and Cellular Neuroscience 84: 132–141. doi: 10.1016/j.mcn.2017.03.003.

Barbier, P., Zejneli, O., Martinho, M., Lasorsa, A., Belle, V., Smet-Nocca, C., Tsvetkov, P.O., Devred, F., Landrieu, I. (2019): Role of Tau as a Microtubule-Associated Protein: Structural and Functional Aspects. Frontiers in Aging Neuroscience 11: 204. doi: 10.3389/fnagi.2019.00204.

Chu, D., Liu, F. (2022): Tau in Health and Neurodegenerative Diseases. In Hippocampus - Cytoarchitecture and Diseases (ed X. Zhang), p. IntechOpen. doi: 10.5772/intechopen.101299.

David, D.C., Layfield, R., Serpell, L., Narain, Y., Goedert, M., Spillantini, M.G. (2002): Proteasomal degradation of tau protein: Tau and the proteasome. Journal of Neurochemistry 83: 176–185. doi: 10.1046/j.1471-4159.2002.01137.x.

Elie, A., Prezel, E., Guérin, C., Denarier, E., Ramirez-Rios, S., Serre, L., Andrieux, A., Fourest-Lieuvin, A., Blanchoin, L., Arnal, I. (2015): Tau co-organizes dynamic microtubule and actin networks. Scientific Reports 5: 9964. doi: 10.1038/srep09964.

Falcon, B., Cavallini, A., Angers, R., Glover, S., Murray, T.K., Barnham, L., Jackson, S., O'Neill, M.J., Isaacs, A.M., Hutton, M.L., Szekeres, P.G., Goedert, M., Bose, S. (2015): Conformation Determines the Seeding Potencies of Native and Recombinant Tau Aggregates. Journal of Biological Chemistry 290: 1049–1065. doi: 10.1074/jbc.M114.589309.

Fan, L., Mao, C., Hu, X., Zhang, S., Yang, Z., Hu, Z., Sun, H., Fan, Y., Dong, Y., Yang, J., Shi, C., Xu, Y. (2020): New Insights Into the Pathogenesis of Alzheimer's Disease. Frontiers in Neurology 10: 1312. doi: 10.3389/fneur.2019.01312.

Fuster-Matanzo, A., Hernández, F., Ávila, J. (2018): Tau Spreading Mechanisms; Implications for Dysfunctional Tauopathies. International Journal of Molecular Sciences 19: 645. doi: 10.3390/ijms19030645.

Gauthier, S., Rosa-Neto, P., Morais, J.A., Webster, C. (2021): World Alzheimer Report 2021: Journey through the diagnosis of dementia. Alzheimer's Disease International, London, England.

Goedert, M. (2020): Tau proteinopathies and the prion concept. In Progress in Molecular Biology and Translational Science pp. 239–259. Elsevier. doi: 10.1016/bs.pmbts.2020.08.003.

Goedert, M., Spillantini, M.G. (2017): Propagation of Tau aggregates. Molecular Brain 10: 18. doi: 10.1186/s13041-017-0298-7.

Guo, T., Noble, W., Hanger, D.P. (2017): Roles of tau protein in health and disease. Acta Neuropathologica 133: 665–704. doi: 10.1007/s00401-017-1707-9.

Hanger, D.P., Anderton, B.H., Noble, W. (2009): Tau phosphorylation: the therapeutic challenge for neurodegenerative disease. Trends in Molecular Medicine 15: 112–119. doi: 10.1016/j.molmed.2009.01.003.

Holmes, B.B., Furman, J.L., Mahan, T.E., Yamasaki, T.R., Mirbaha, H., Eades, W.C., Belaygorod, L., Cairns, N.J., Holtzman, D.M., Diamond, M.I. (2014): Proteopathic tau seeding predicts tauopathy in vivo. Proceedings of the National Academy of Sciences 111: E4376–E4385. doi: 10.1073/pnas.1411649111.

Hrubý, J. (2020): Autophagy induction decreases the presence of endogenous P301S tau aggregates. Bachelor thesis, Palacký University Olomouc, Faculty of Science, Olomouc.

Jeganathan, S., von Bergen, M., Brutlach, H., Steinhoff, H.-J., Mandelkow, E. (2006): Global Hairpin Folding of Tau in Solution. Biochemistry 45: 2283–2293. doi: 10.1021/bi0521543.

Kametani, F., Yoshida, M., Matsubara, T., Murayama, S., Saito, Y., Kawakami, I., Onaya, M., Tanaka, H., Kakita, A., Robinson, A.C., Mann, D.M.A., Hasegawa, M. (2020): Comparison of Common and Disease-Specific Post-translational Modifications of Pathological Tau Associated With a Wide Range of Tauopathies. Frontiers in Neuroscience 14: 581936. doi: 10.3389/fnins.2020.581936.

Koudelková, Mud.M. (2009): Praktické zkušenosti s laboratorní diagnostikou Alzheimerovy nemoci pomocí tau proteinu, fosfo-tau proteinu a beta amyloidu v likvoru. Neurologie pro praxi 10: 290–293.

Lathuiliere, A., Hyman, B.T. (2021): Quantitative Methods for the Detection of Tau Seeding Activity in Human Biofluids. Frontiers in Neuroscience 15: 654176. doi: 10.3389/fnins.2021.654176.

Lee, M.J., Lee, J.H., Rubinsztein, D.C. (2013): Tau degradation: The ubiquitin–proteasome system versus the autophagy-lysosome system. Progress in Neurobiology 105: 49–59. doi: 10.1016/j.pneurobio.2013.03.001.

Liang, S.-Y., Wang, Z.-T., Tan, L., Yu, J.-T. (2022): Tau Toxicity in Neurodegeneration. Molecular Neurobiology 59: 3617–3634. doi: 10.1007/s12035-022-02809-3.

Liu, F., Grundke-Iqbal, I., Iqbal, K., Gong, C.-X. (2005): Contributions of protein phosphatases PP1, PP2A, PP2B and PP5 to the regulation of tau phosphorylation. European Journal of Neuroscience 22: 1942–1950. doi: 10.1111/j.1460-9568.2005.04391.x.

Magnani, E., Fan, J., Gasparini, L., Golding, M., Williams, M., Schiavo, G., Goedert, M., Amos, L.A., Spillantini, M.G. (2007): Interaction of tau protein with the dynactin complex. The EMBO Journal 26: 4546–4554. doi: 10.1038/sj.emboj.7601878.

Mietelska-Porowska, A., Wasik, U., Goras, M., Filipek, A., Niewiadomska, G. (2014): Tau Protein Modifications and Interactions: Their Role in Function and Dysfunction. International Journal of Molecular Sciences 15: 4671–4713. doi: 10.3390/ijms15034671.

Mirbaha, H., Chen, D., Morazova, O.A., Ruff, K.M., Sharma, A.M., Liu, X., Goodarzi, M., Pappu, R.V., Colby, D.W., Mirzaei, H., Joachimiak, L.A., Diamond, M.I. (2018): Inert and seed-competent tau monomers suggest structural origins of aggregation. eLife 7: e36584. doi: 10.7554/eLife.36584.

Morris, M., Maeda, S., Vossel, K., Mucke, L. (2011): The Many Faces of Tau. Neuron 70: 410–426. doi: 10.1016/j.neuron.2011.04.009.

Mueller, R.L., Combs, B., Alhadidy, M.M., Brady, S.T., Morfini, G.A., Kanaan, N.M. (2021): Tau: A Signaling Hub Protein. Frontiers in Molecular Neuroscience 14: 647054. doi: 10.3389/fnmol.2021.647054.

Mukrasch, M.D., Bibow, S., Korukottu, J., Jeganathan, S., Biernat, J., Griesinger, C., Mandelkow, E., Zweckstetter, M. (2009): Structural Polymorphism of 441-Residue Tau at Single Residue Resolution. PLoS Biology 7: e1000034. doi: 10.1371/journal.pbio.1000034.

Muralidar, S., Ambi, S.V., Sekaran, S., Thirumalai, D., Palaniappan, B. (2020): Role of tau protein in Alzheimer's disease: The prime pathological player. International Journal of Biological Macromolecules 163: 1599–1617. doi: 10.1016/j.ijbiomac.2020.07.327.

Neve, R.L., Harris, P., Kosik, K.S., Kurnit, D.M., Donlon, T.A. (1986): Identification of cDNA clones for the human microtubule-associated protein tau and chromosomal localization of the genes for tau and microtubule-associated protein 2. Molecular Brain Research 1: 271–280. doi: 10.1016/0169-328X(86)90033-1.

Poppek, D., Keck, S., Ermak, G., Jung, T., Stolzing, A., Ullrich, O., Davies, K.J.A., Grune, T. (2006): Phosphorylation inhibits turnover of the tau protein by the proteasome: influence of *RCAN1* and oxidative stress. Biochemical Journal 400: 511–520. doi: 10.1042/BJ20060463.

Rico, T., Gilles, M., Chauderlier, A., Comptdaer, T., Magnez, R., Chwastyniak, M., Drobecq, H., Pinet, F., Thuru, X., Buée, L., Galas, M.-C., Lefebvre, B. (2021): Tau Stabilizes Chromatin Compaction. Frontiers in Cell and Developmental Biology 9: 740550. doi: 10.3389/fcell.2021.740550.

Seidler, P.M., Boyer, D.R., Murray, K.A., Yang, T.P., Bentzel, M., Sawaya, M.R., Rosenberg, G., Cascio, D., Williams, C.K., Newell, K.L., Ghetti, B., DeTure, M.A., Dickson, D.W., Vinters, H.V., Eisenberg, D.S. (2019): Structure-based inhibitors halt prion-like seeding by Alzheimer's disease–and tauopathy–derived brain tissue samples. Journal of Biological Chemistry 294: 16451–16464. doi: 10.1074/jbc.RA119.009688.

Takei, Y., Teng, J., Harada, A., Hirokawa, N. (2000): Defects in axonal elongation and neuronal migration in mice with disrupted tau and map1b genes. The Journal of Cell Biology 150: 989–1000. doi: 10.1083/jcb.150.5.989.

Ye, H., Han, Y., Li, P., Su, Z., Huang, Y. (2022): The Role of Post-Translational Modifications on the Structure and Function of Tau Protein. Journal of Molecular Neuroscience. doi: 10.1007/s12031-022-02002-0.

Zeng, Y., Yang, J., Zhang, B., Gao, M., Su, Z., Huang, Y. (2021): The structure and phase of tau: from monomer to amyloid filament. Cellular and Molecular Life Sciences 78: 1873–1886. doi: 10.1007/s00018-020-03681-x.

Zhang, X., Gao, F., Wang, D., Li, C., Fu, Y., He, W., Zhang, J. (2018): Tau Pathology in Parkinson's Disease. Frontiers in Neurology 9: 809. doi: 10.3389/fneur.2018.00809.